

Assessment of Sodium Thermal Stratification Models Utilizing the TSTF Benchmark

Nuclear Science and Engineering Division

About Argonne National Laboratory

Argonne is a U.S. Department of Energy laboratory managed by UChicago Argonne, LLC under contract DE-AC02-06CH11357. The Laboratory's main facility is outside Chicago, at 9700 South Cass Avenue, Argonne, Illinois 60439. For information about Argonne and its pioneering science and technology programs, see www.anl.gov.

DOCUMENT AVAILABILITY

Online Access: U.S. Department of Energy (DOE) reports produced after 1991 and a growing number of pre-1991 documents are available free at OSTI.GOV (<http://www.osti.gov/>), a service of the US Dept. of Energy's Office of Scientific and Technical Information.

Reports not in digital format may be purchased by the public from the National Technical Information Service (NTIS):

U.S. Department of Commerce
National Technical Information Service
5301 Shawnee Rd
Alexandria, VA 22312
www.ntis.gov
Phone: (800) 553-NTIS (6847) or (703) 605-6000
Fax: (703) 605-6900
Email: orders@ntis.gov

Reports not in digital format are available to DOE and DOE contractors from the Office of Scientific and Technical Information (OSTI):

U.S. Department of Energy
Office of Scientific and Technical Information
P.O. Box 62
Oak Ridge, TN 37831-0062
www.osti.gov
Phone: (865) 576-8401
Fax: (865) 576-5728
Email: reports@osti.gov

Disclaimer

This report was prepared as an account of work sponsored by an agency of the United States Government. Neither the United States Government nor any agency thereof, nor UChicago Argonne, LLC, nor any of their employees or officers, makes any warranty, express or implied, or assumes any legal liability or responsibility for the accuracy, completeness, or usefulness of any information, apparatus, product, or process disclosed, or represents that its use would not infringe privately owned rights. Reference herein to any specific commercial product, process, or service by trade name, trademark, manufacturer, or otherwise, does not necessarily constitute or imply its endorsement, recommendation, or favoring by the United States Government or any agency thereof. The views and opinions of document authors expressed herein do not necessarily state or reflect those of the United States Government or any agency thereof, Argonne National Laboratory, or UChicago Argonne, LLC.

Assessment of Sodium Thermal Stratification Models Utilizing the TSTF Benchmark

Prepared by

Yeongshin Jeong, Matthew Bucknor, Tyler Sumner, Daniel J. O'Grady, Acacia J. Brunett
Nuclear Science and Engineering, Argonne National Laboratory

Prepared for Sodium Demonstration project – Methods Development
CRADA 2021-21076

April 2023

REVIEW AND APPROVAL

Prepared by: *Yeongshin Jeong* Date: 04/28/2023
Yeongshin Jeong

Reviewed by: *Matthew Bucknor* Date: 04/28/2023
Matthew Bucknor

Approved by: *Tanju Sofu* Date: 5/8/2023
Tanju Sofu

REVISION HISTORY

Revision No.	Effective Date	Section(s) Affected	Description of Change(s)
0	2023-04-28	All	Initial release.

ABSTRACT

As a result of certain transient scenarios, a thermally stratified layer of liquid sodium can develop in the bulk coolant volumes of a sodium-cooled fast reactor (SFR). In addition to the effects a stratification layer has on the temperature of the heat transport system, a stratification layer can also influence the transition to and establishment of natural circulation flow, which plays an important role in passive cooling and the inherent safety of a pool-type SFR. Therefore, the ability to accurately capture thermal stratification phenomena is important when demonstrating the safety basis of a pool-type SFR during transient sequences.

The present work assesses various computational models with different fidelities in their ability to predict thermal stratification in the upper plenum of an SFR. Each computational model will be assessed using the data generated at the Thermal Stratification Test Facility (TSTF) located at the University of Wisconsin-Madison. Using measured flow rate and inlet temperature data, the measured temperature distributions of the tests are compared to the predictions of the lumped-volume-based models in SAS4A/SASSYS-1, a 1D-based model in SAM, and a 3-D computational fluid dynamics (CFD) model using STAR-CCM+. The relative performance of the various computational methods is assessed with respect to key metrics such as bulk coolant temperature distribution and plenum exit temperature. A total of eight tests are analyzed, covering different combinations of flow rates (3 and 10 GPM) and upper internal structure (UIS) configurations (none, solid, porous, and open)

The perfect mixing model of SAS4A/SASSYS-1 provides the highest accuracy when the flow rate is high and there is no UIS in the test vessel, as high flow rate injection promotes thermal mixing of the sodium in the test vessel. For most of the analyzed tests, the stratified volume model of SAS4A/SASSYS-1 is able to predict the delay in the outlet temperature drop and temperature distribution in the test vessel by a small number of layers to represent thermal stratification. However, the stratified volume model can only simulate a maximum of three temperature layers within a volume and when a layer approaches the elevation of the outlet, the predicted outlet temperature can demonstrate rapid, non-physical changes. The 1-D axial mixing model of SAM provides results that agree reasonably well with the measured data in the prediction of the temporal evolution of the outlet temperature with the exception of the case with a high flow rate and no UIS. The SAM 1-D model has a similar level of accuracy to CFD results when it comes to predicting the outlet temperature. CFD shows overall good agreement in predicting the temperature distribution in the test vessel and outlet temperature. As CFD can model the test vessel geometry in detail, it performs well in the cases of complex geometries such as tests that included a UIS and internal flow through the UIS resulting in active mixing of the coolant in the test vessel.

Each of the models discussed in the present work has the potential to be useful during the various stages of reactor design, analysis, and licensing. The lumped-volume approach can be applied for fast turnaround safety calculations to obtain overall reactor behavior during transients. The 1-D models provide improved accuracy when stratification is expected for a relatively low increase in the computational cost. The CFD model can be utilized for confirmatory analysis of the 1-D model, when experimental measurements are not available.

TABLE OF CONTENTS

Abstract.....	iii
Table of Contents	iv
List of Figures.....	v
List of Tables	vii
1 Introduction.....	1
2 TSTF Benchmark.....	2
3 Thermal Stratification Models	4
3.1 Stratified Volume Model of SAS4A/SASSYS-1	4
3.2 1-D Axial Mixing Model of SAM.....	6
3.3 Unsteady RANS model of CFD	6
4 Computational Models of TSTF	8
4.1 Model Assumptions, Material Properties, and Boundary Conditions	8
4.2 SAS4A/SASSYS-1 Model	9
4.2.1 Parametric Sensitivity of Stratified Volume Model of SAS4A/SASSYS-1	12
4.3 SAM Model	14
4.3.1 Parametric Sensitivity of 1-D Axial Mixing Model of SAM	14
4.4 CFD Model.....	16
5 Results and Discussions	17
5.1 TSTF Benchmark Results.....	17
5.2 Discussions on Thermal Stratification Models.....	32
Acknowledgement.....	34
References	35
Appendix	36

LIST OF FIGURES

Figure 1 TSTF layout and its test section for various UIS configurations [3]	2
Figure 2 TSTF test vessel temperature distributions measured by FOTS [3]	3
Figure 3 Stratified volume staged in SAS4A/SASSYS-1 [5]	4
Figure 4 Boundary conditions for the selected TSTF tests	9
Figure 5 The TSTF PRIMAR-4 model	11
Figure 6 Parametric sensitivities of no UIS cases with respect to XLENTR and EPSTST	12
Figure 7 Parametric sensitivities of solid UIS cases with respect to XLENTR, EPSTST and inlet orientation.....	13
Figure 8 The TSTF test vessel SAM model	14
Figure 9 Parametric sensitivity of the 1-D axial mixing model of SAM.	15
Figure 10 Mesh of the TSTF CFD model	16
Figure 11 Temperature distribution in the test vessel using SAS4A/SASSYS-1 – No UIS cases.....	17
Figure 12 Temperature distribution in the test vessel using SAS4A/SASSYS-1 – Solid UIS cases.....	18
Figure 13 Temperature distribution in the test vessel using SAS4A/SASSYS-1 – Variable UIS, $\alpha=4\%$ cases	18
Figure 14 Temperature distribution in the test vessel using SAS4A/SASSYS-1 – Variable UIS, $\alpha=100\%$ cases	18
Figure 15 Comparison of sodium temperature distribution in the test vessel (SAS4A/SASSYS-1) – no UIS cases	19
Figure 16 Comparison of sodium temperature distribution in the test vessel (SAS4A/SASSYS-1) – Solid UIS cases.....	19
Figure 17 Comparison of sodium temperature distribution in the test vessel (SAS4A/SASSYS-1) – Variable UIS, $\alpha=4\%$ cases	20
Figure 18 Comparison of sodium temperature distribution in the test vessel (SAS4A/SASSYS-1) – Variable UIS, $\alpha=100\%$ cases	20
Figure 19 Comparison of temperature distribution in the test vessel (SAM) – no UIS cases.....	21
Figure 20 Comparison of temperature distribution in the test vessel (SAM) – solid UIS cases.....	21
Figure 21 Comparison of temperature distribution in the test vessel (SAM) – variable UIS, $\alpha=4\%$ cases.....	21
Figure 22 Comparison of temperature distribution in the test vessel (SAM) – variable UIS, $\alpha=100\%$ cases.....	22
Figure 23 Comparison of temperature distribution in the test vessel (CFD) – no UIS cases.....	23
Figure 24 Comparison of temperature distribution in the test vessel (CFD) – solid UIS cases.....	23
Figure 25 Comparison of temperature distribution in the test vessel (CFD) – variable UIS, $\alpha=4\%$ cases.....	23
Figure 26 Comparison of temperature distribution in the test vessel (CFD) – variable UIS, $\alpha=100\%$ cases.....	24
Figure 27 Snapshots of sodium temperature distribution in the test vessel using CFD.	24
Figure 28 Comparisons of the test vessel outlet temperature results of TSTF benchmark – no UIS.....	25

Figure 29 Comparisons of the test vessel outlet temperature results of TSTF benchmark – solid UIS	26
Figure 30 Comparisons of the test vessel outlet temperature results of TSTF benchmark – variable UIS, $\alpha=4\%$	26
Figure 31 Comparisons of the test vessel outlet temperature results of TSTF benchmark – variable UIS, $\alpha=100\%$	27
Figure 32 Time-averaged RMS error and local min/max deviations of no UIS cases	29
Figure 33 Time-averaged RMS error and local min/max deviations of solid UIS cases	29
Figure 34 Time-averaged RMS error and local min/max deviations of various UIS, $\alpha=4\%$ cases.....	29
Figure 35 Time-averaged RMS error and local min/max deviations of various UIS, $\alpha=100\%$ cases.....	30

LIST OF TABLES

Table I. Selective TSTF tests for benchmarking	2
Table II Key parameters for the core model of the SAS4A/SASSYS-1 TSTF model.....	10
Table III TSTF PRIMAR-4 model components.....	11
Table IV. Test matrix for parametric sensitivity of the 1-D axial mixing model of SAM.....	15
Table V Summary of the TSTF benchmark by fidelity levels and their qualitative performance	32
Table VI A list of the parameters in the script used for sensitivity analysis	36

1 Introduction

In a sodium-cooled fast reactor (SFR), thermal stratification of a bulk coolant volume such as the cold pool can occur when the coolant entering a volume is at a significantly different temperature from that of the volume itself. These conditions can occur in low power transients or a protected loss of flow event, which can induce a large temperature gradient of the liquid sodium in the pool. In some events, when both the flow rate and the core outlet temperature decrease, buoyancy forces may modify the flow pattern in the upper plenum and thermal stratification can occur near the inlet of the intermediate heat exchanger (IHX) [1]. In addition to the effects of the stratification on the heat transport system temperature distribution, stratification can also influence the transition to and establishment of natural circulation of the coolant, which plays an important role in the passive cooling and inherent safety of a pool-type SFR. Therefore, it is important to accurately represent thermal stratification phenomena when demonstrating the safety basis of a pool-type SFR during transient sequences.

In this work, modeling and simulation of thermal stratification has been performed with various fidelities, including a 0-D system-level approach, a 1-D model approach and a 3-D approach. The system-level method provides highly approximated results via relatively fast calculations, while the 3-D methods offer reasonably informative results in predicting phenomena but require large computational costs. The 1-D models have also been developed as a compromise between the major drawbacks of the aforementioned two methods. Each model, which utilizes a different fidelity level, has the potential to be useful during the various stages of reactor design, analysis, and licensing, where the ultimate role and utility of the model would be dependent on the desired analysis fidelity and computational resources available.

To explore the capabilities and features of the various models in predicting bulk coolant thermal stratification, tests performed at the Thermal Stratification Test Facility (TSTF) [2] were simulated. The TSTF was designed and built at the University of Wisconsin-Madison to investigate the thermal stratification phenomena of liquid sodium in SFR upper plena. It was operated to provide spatial and temporal temperature data in finer resolution than previous experiments using advanced instrumentations such as distributed fiber optic temperature sensors (FOTS). The TSTF benchmark specification defines the system geometry and conditions necessary to model and simulate the selected sodium stratification tests [3].

In this work, representative computational models of different fidelities are assessed by comparing temperature simulation results to TSTF experimental data. The relative performance of the various computational methods for predicting thermal stratification are discussed with respect to key metrics such as bulk coolant temperature distribution and plenum exit temperature. The advantages and limitations of each software tool (and fidelity level) are then assessed based on their general ability to simulate the different TSTF experiments.

2 TSTF Benchmark

The tests included in the TSTF benchmark are forced flow tests where colder sodium is injected at a fixed rate into the test section, which is pre-heated such that it contains relatively hotter sodium. The colder sodium is pumped from a supply reservoir into the test section. Sodium exiting the test section is pumped into a holding tank to ensure it does not mix with the sodium in the supply reservoir and a constant test section inlet temperature is maintained throughout the experiment. The test section of the TSTF contains a removeable upper internal structure (UIS) with adjustable flow-through configurations, where a variable orifice plate can be used to restrict flow area by various fractions. The variable flow area restriction is defined as α , the ratio of the allowed flow area through the UIS to the internal cross-sectional area of the UIS, as shown in Figure 1. From the TSTF experimental test matrix, eight tests are assessed in this work (shown in Table I). Cases were chosen such that the experimental configurations and domains were bounded, that is, two representative cases for bounding UIS configurations with low and high inlet flow rates along with tests where the UIS was removed. For all tests, sodium at 200°C from the test supply reservoir flows into the test section, which is initially at 300°C. The temperature inside the test vessel was measured by FOTS and thermocouples. The axial temperature distribution of the temperature as a function of time for each of the eight experiments is shown in Figure 2.

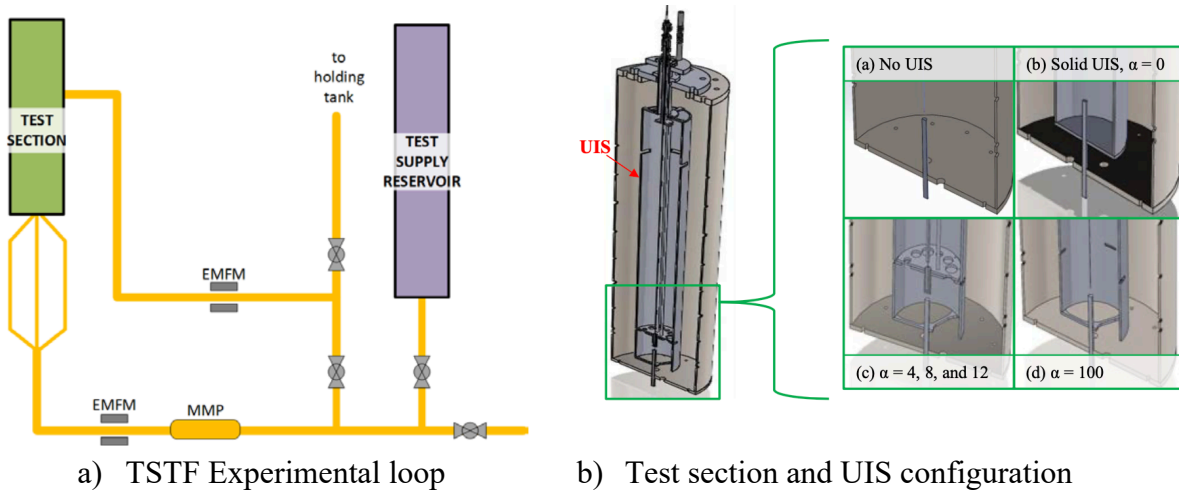


Figure 1 TSTF layout and its test section for various UIS configurations [3]

Table I. Selective TSTF tests for benchmarking

Exp No.	UIS Configurations	Flow rate [gpm]
129	No UIS	3
133		10
224	Solid UIS	3
227		10
273	Variable UIS – $\alpha=4$ %	3
270		10
277	Variable UIS – $\alpha=100$ %	3
283		10

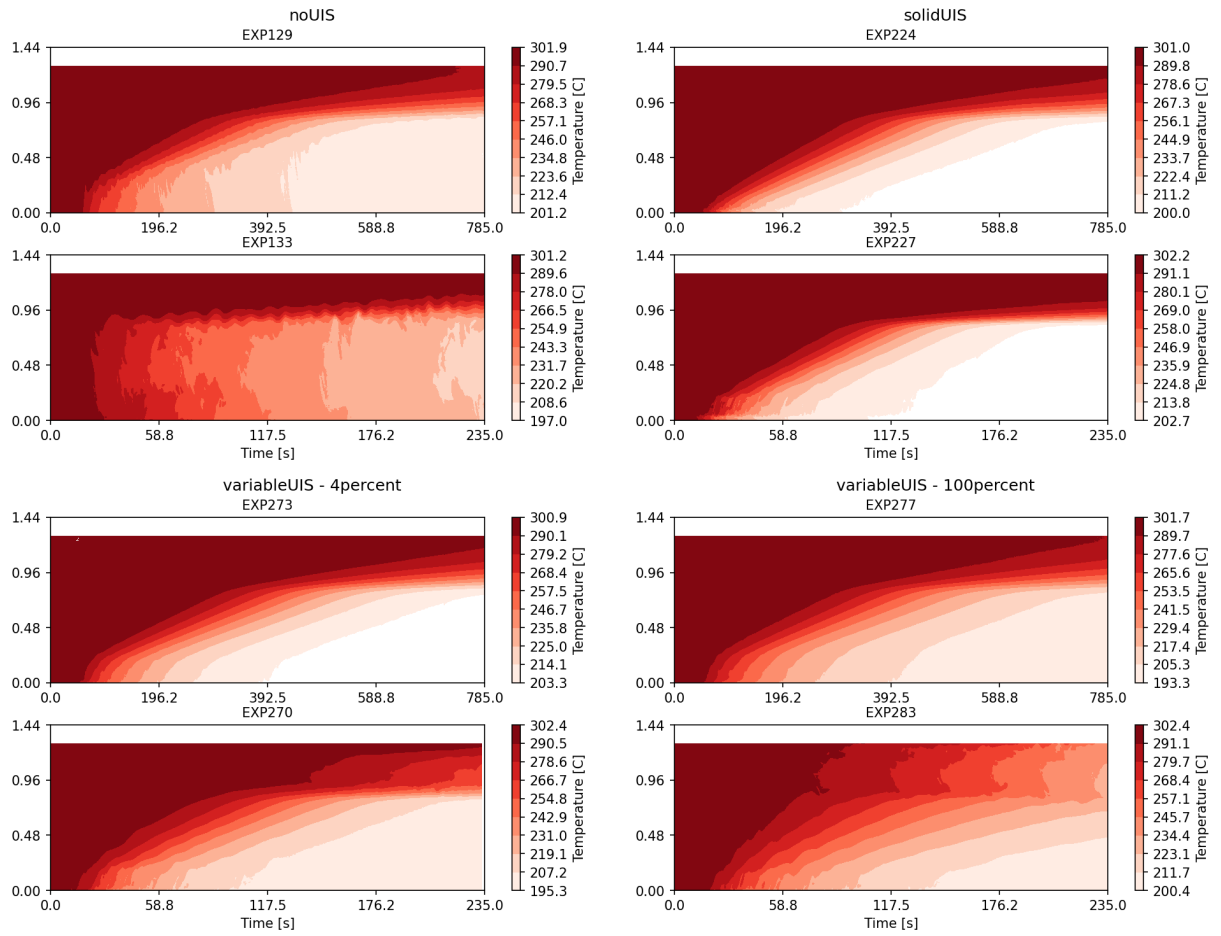


Figure 2 TSTF test vessel temperature distributions measured by FOTS [3]

3 Thermal Stratification Models

A number of different computational models have been developed to predict the thermal stratification phenomenon. A comprehensive overview of the different approaches is available in [4]. Among the different models, this work focuses on lumped-volume-based models in SAS4A/SASSYS-1 [5], a 1-D model in the System Analysis Module (SAM) [6], and 3-D computational fluid dynamics (CFD) using STAR-CCM+ [8]. This section describes the models of each software tool.

3.1 Stratified Volume Model of SAS4A/SASSYS-1

The SAS4A/SASSYS-1 computer code is a system-level code developed by Argonne National Laboratory for thermal-hydraulic and neutronic analyses of power and flow transients in liquid metal-cooled reactors [5]. The thermal-hydraulic solver, PRIMAR-4, of SAS4A/SASSYS-1 contains a perfect mixing model and a stratified volume model for the liquid temperature in a compressible volume. The perfect mixing model calculates an average liquid temperature for a compressible volume, while the stratified volume model can approximate the development and propagation of stratified layers with representative temperatures and time-dependent thicknesses.

The stratified volume model builds on the code PLENUM-2A [9], which includes a small number of distinct temperature regions in the coolant with different stages in the calculation, a plume height correlation, and a correlation for interface movement due to entrainment of a hot layer into a colder plume rising from the core outlet. The current stratified volume model has been extended from the PLENUM-2A implementation to handle up and down flow transients and horizontal discharges. It calculates the formation, dissipation, and elevation changes of the interfaces and layer temperatures for up to three regions in five stages, where these regions and stages are dependent on temperatures and velocities of the jet and the pool. Figure 3 shows the various stages and cases considered in the stratified volume model of SAS4A/SASSYS-1, which are representative of the cases where the core outlet temperature drops below the outlet plenum temperature.

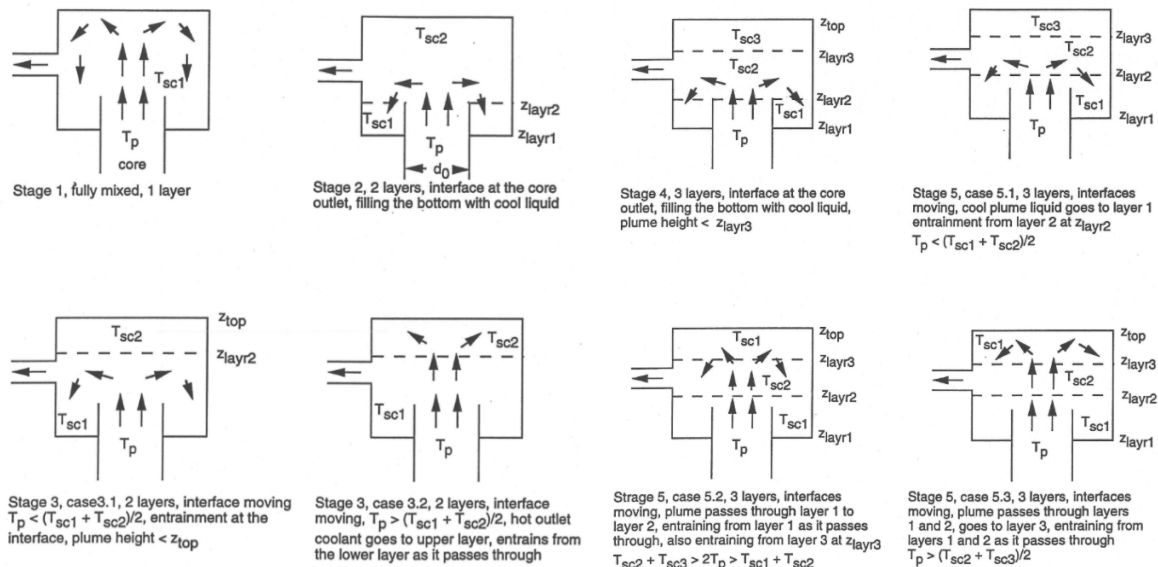


Figure 3 Stratified volume staged in SAS4A/SASSYS-1 [5]

When the jet can penetrate to the top of the pool and the jet temperature is relatively close to the pool temperature, the pool is fully mixed resulting in the configuration shown in stage 1. If the jet temperature is lower than that of the pool and has insufficient momentum, the jet might no longer be able to penetrate to the top of the plenum, which leads to the development of stratification. Depending on the momentum and temperature of the jet, thermal stratification can begin in stage 2 or stage 3. In stage 2, two layers exist in the pool, and the interface between layers is below the plenum outlet. Effectively, stage 2 captures the scenarios where the coolant entering the pool sinks to a lower elevation immediately. In stage 3, the jet has the momentum and/or temperature needed to rise above the entrance of the pool and entrain some of the surrounding fluid. The jet may remain in the first layer, case 3.1, or penetrate into the second layer, case 3.2. In the case of a vertically discharged jet, if the temperature/momentum of the jet continues to decrease, a third layer may be formed below the entrance of the pool, stage 4. As the temperature or momentum of the jet and the temperature of the 3 layers changes, stage 5 is entered. Shown in stage 5, case 5.1, the jet entrains fluid from layer 2 and enters layer 1. Shown in stage 5, case 5.2, the jet entrains fluid from layers 1 and 3 and finishes in layer 2. Shown in stage 5, case 5.3, the jet entrains fluid from layers 1 and 2 and finishes in layer 3. For the horizontal jet, only stages 1, 3, and 5 are possible. Layers in each stage are collapsed if the mass in the layer falls below a threshold. For a given time step, the stage of the model is determined by the conditions of the jet and the pool based on the model parameters calculated in the stratified volume model.

The jet height (h_{jet} [m]) determined from a correlation given by Yang [10] as a function of Froude number (Fr) is shown in equation (1), where ρ_{jet} is the density of the jet [kg/m^3], g is the gravitational acceleration [m^2/s], and ρ_{pool} is the density of the pool [kg/m^3]. Given the jet height value, the entrainment rate at an interface (w_{ent} [kg/s]) is obtained from a correlation by Lorenz and Howard [9] as shown in equation (2) for conditions when the jet is colder than the pool. The entrainment rate of a hotter jet is calculated by equation (3), which describes flow through a cool liquid layer of a thickness (dz [m]) with a flow rate (W_h [kg/s]), where L_{ent} is the user-defined entrainment length [m]. The velocity and diameter of the jet (D_j [m] and V_j [m/s]) are calculated based on the elevation change from the core outlet (z_o [m]) obtained by equation (4), where r_o is the core outlet radius [m], depending on whether the interface occurs within the zone of flow establishment (when $z < z_o$) or in the zone of established flow (when $z > z_o$) as expressed in equations (5) or (6).

$$h_{jet} = 1.0484Fr^{0.785}, \text{ where } Fr = v_o^2 \rho_{jet} / [gr_o^2 (\rho_{jet} - \rho_{pool})] \quad (1)$$

$$w_{ent} = 0.2\pi\rho_{jet}V_jD_j^2Fr^{-1.1} \quad (2)$$

$$w_{ent} = \frac{dz}{L_{ent}}W_h \quad (3)$$

$$z_o = r_o/0.111 \quad (4)$$

$$\frac{v_j}{v_o} = \begin{cases} 0.25 + 0.02095(z/d_o) + 0.003969(z/d_o)^2 & z < z_o \\ 2.018/(z/d_o) & z > z_o \end{cases} \quad (5)$$

$$\frac{d_j}{d_o} = \begin{cases} 1 + 0.2104(z/d_o) & z < z_o \\ 0.8649(z/d_o) & z > z_o \end{cases} \quad (6)$$

3.2.1-D Axial Mixing Model of SAM

The SAM code [6] is a system analysis tool developed at Argonne National Laboratory built on the MOOSE framework [7] allowing for the flexible modeling of various advanced reactor concepts. SAM provides a number of different 0-D and 1-D components that can be used to capture the heat structures and flow fields in advanced reactors. For more complex geometries, including pebble bed and molten salt reactor cores, SAM has the ability to represent the system in 2-D or 3-D. For thermal mixing and stratification in large enclosures, the SAM code supports a 1-D modeling approach, modeling inter-volume energy exchange by advection and flow mixing. The 1-D axial mixing model [11] solves the one-dimensional fluid conversion equation as shown in equation (7), where ρ is the fluid density [kg/m^3], H is the fluid enthalpy [J], u is the fluid velocity [m/s], k is the fluid thermal conductivity [W/mK], T is the fluid temperature [K], and G_{mix} is the mixing mass flux [$\text{kg}/\text{m}^2\text{s}$].

The governing equation for the mixing velocity (u_m [m/s]) originates from the momentum conservation equation but was derived from the energy conservation equation shown in equation (8), where μ is the fluid viscosity [Pa s], c_f is the friction coefficient multiplier [-], f is the friction loss coefficient [-], D is the hydraulic diameter [m], β is the thermal expansion coefficient of the fluid [1/K], C_{gb} is the coefficient for the buoyancy effects in the specific geometry [-], and C_{gv} is the coefficient for the velocity effects in the specific geometry [-]. It includes the transport terms on the left side of the equation and the diffusion term, the resistance term, and the source terms in sequential order on the right side of the equation (8). Flow mixing is mainly driven by the local flow velocity, geometry, and buoyancy effect with the two parameters C_{gb} and C_{gv} . The 1-D axial mixing model has been verified and tested for various cases, showing its applicability to simulate the transient behavior in SFR pools with fair accuracy and efficiency [11].

$$\frac{\partial(\rho H)}{\partial t} + \frac{\partial((\rho u + G_{\text{mix}})H)}{\partial z} = \nabla(k\nabla T), \text{ where } G_{\text{mix}} = \rho u_m \quad (7)$$

$$\frac{\partial(\rho u_m)}{\partial t} + \frac{\partial(\rho u u_m)}{\partial z} = \mu \nabla^2 u_m + \frac{c_f f}{2D} \rho u_m^2 + C_{gb} \beta \rho g \nabla T - \frac{c_f f}{2D} \rho (C_{gv} u)^2 \quad (8)$$

3.3 Unsteady RANS model of CFD

The present study utilized the 3-D CFD software STAR-CCM+ [8]. CFD has been the widely used in various applications due to its strong performance in many flow cases. The present study utilized the unsteady Reynolds Averaged Navier Stokes (RANS) turbulence modeling approach due to its practicality, as direct numerical simulation (DNS) or large eddy simulation (LES) methods are too computationally expensive for routine use. Incorporating 3-D geometries and the buoyancy effect, unsteady RANS (URANS) has been used to predict complex mixing phenomena such as thermal stratification. The unsteady Reynolds averaged energy equation is shown in equation (9) [8], where $\bar{\mathbf{v}}$ is the mean velocity [m/s], \bar{p} is the mean pressure [Pa], $\bar{\mathbf{T}}$ is the mean viscous stress tensor [N/m^2], \mathbf{f}_b is the body force term [N], \bar{E} is the mean total energy per unit mass [J/kg], and $\bar{\mathbf{q}}$ is the mean heat flux [W/m^2].

$$\frac{\partial(\rho\bar{E})}{\partial t} + \nabla \cdot (\rho\bar{E}\bar{\mathbf{v}}) = -\nabla \cdot \bar{p}\bar{\mathbf{v}} + \nabla \cdot (\bar{\mathbf{T}} + \bar{\mathbf{T}}_{RANS})\bar{\mathbf{v}} - \nabla \cdot \bar{\mathbf{q}} + \mathbf{f}_b\bar{\mathbf{v}} \quad (9)$$

For the RANS turbulence model, the mean heat flux in the energy equation is based on the Boussinesq approximation [8] expressed with a turbulent eddy viscosity and a turbulent Prandtl number as shown in equation (10), where k is the thermal conductivity of the fluid [W/mK], μ_t is the turbulent eddy viscosity [m²/s], C_p is the specific heat [J/kgK], Pr_t is the turbulent Prandtl number [-], and \bar{T} is the mean temperature [K]. The turbulent Prandtl number is commonly assumed to be 0.9 in practice, which has resulted in adequate temperature predictions for a wide range of conditions [12]. The turbulent eddy viscosity is given by the respective turbulence model, which solves the transport equations for the turbulent kinetic energy and turbulent dissipation rate.

$$\bar{\mathbf{q}} = -\left(k + \frac{\mu_t C_p}{Pr_t}\right) \nabla \bar{T} \quad (10)$$

4 Computational Models of TSTF

In this section, the computational models used to simulate the TSTF experiments are presented along with sensitivity studies of major input parameters. Modeling assumptions and boundary conditions from the TSTF benchmark specification are described. Next, details for each of the computational models are presented. Finally, a selection of results from parameter sensitivity studies performed for the SAS4A/SASSYS-1 stratified volume model and the SAM 1-D axial mixing model are provided.

4.1 Model Assumptions, Material Properties, and Boundary Conditions

The TSTF benchmark specification provides the dimensions for the test vessel and mass flow rates and temperatures of sodium flowing into the test section specified as transient boundary conditions for each test.

Several modeling assumptions were made for the TSTF computational models. First, the regions of the TSTF before and after the test section were modeled only as necessary with simplified or approximated dimensions. A complete loop with approximated dimensions was specified for the SAS4A/SASSYS-1 model. The SAM and CFD models include limited geometries for the regions immediately upstream and downstream of the test section, with boundary conditions specified at the test section inlets and outlets. Second, the test vessel was assumed to be well insulated during the tests; thus, solid parts of the test vessel were neglected in the models by setting adiabatic boundary conditions if required. Lastly, because measured flow rates through the UIS were not recorded, and are therefore not available for comparison, the SAS4A/SASSYS-1 and SAM models excluded modeling a separate flow path through the UIS. The SAS4A/SASSYS-1 and SAM results for the variable UIS cases were simulated using the test section geometry corresponding to the solid UIS cases.

The transient boundary conditions of the test section inlet temperature and flow rate were provided in the TSTF benchmark specification. For the SAS4A/SASSYS-1 and SAM models, they were defined using select points that represent the experimental conditions. The inlet temperature and flow rate are provided as input tables. For STAR-CCM+, transient boundary conditions were imported using CSV files as provided and set for inlet boundary conditions for the temperature and velocity interpolated by time step. Figure 4 compares the measure inlet flow rate and temperature with the selected boundary condition data points for two representative tests.

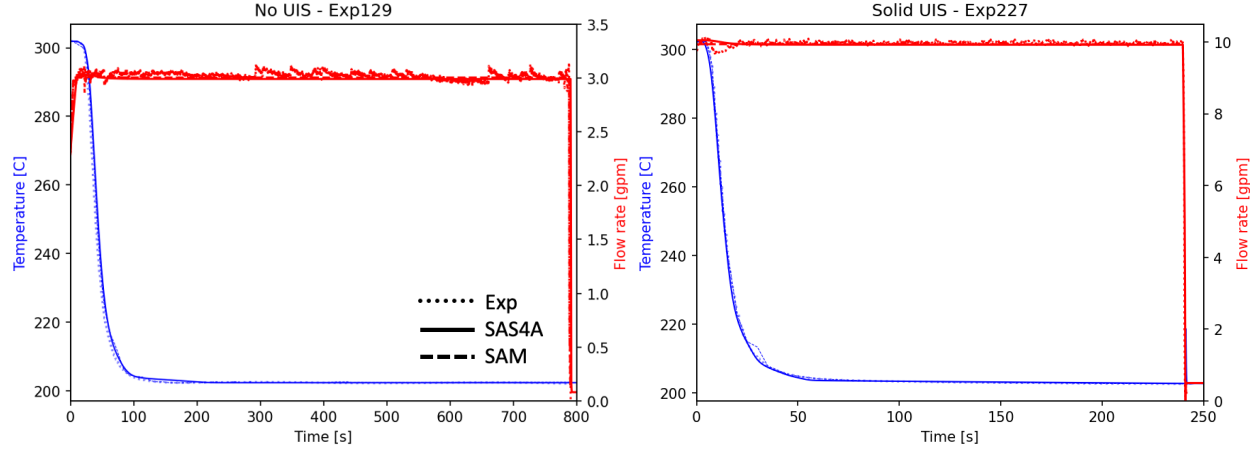


Figure 4 Boundary conditions for the selected TSTF tests

For all models, the SAS4A/SASSYS-1 built-in liquid sodium property correlations were used [5]. This includes the following correlations for liquid sodium density (ρ_l [kg/m³]), specific heat ($C_{p,l}$ [J/kg·K]), thermal conductivity (k [W/m·K]), and viscosity (μ_l [Pa s]):

$$\rho_l = 1.00423 \times 10^3 - 0.21390 \cdot T - 1.1046 \times 10^{-5} \cdot T^2 \quad (11)$$

$$C_{p,l} = \frac{7.3898 \times 10^5}{(T_c - T)^2} + \frac{3.1514 \times 10^5}{T_c - T} + 1.1340 \times 10^3 - 2.2153 \times 10^{-1} \cdot (T_c - T) + 1.1156 \times 10^{-4} \cdot (T_c - T)^2, \text{ where } T_c = 2503.3 \text{ K} \quad (12)$$

$$k_l = 1.1045 \times 10^2 - 6.5112 \times 10^{-2} \cdot T + 1.5430 \times 10^{-5} \cdot T^2 - 2.4617 \times 10^{-9} \cdot T^3 \quad (13)$$

$$\mu_l = 3.6522 \times 10^{-5} + \frac{0.16626}{T} - \frac{4.56877 \times 10^1}{T^2} + \frac{2.8733 \times 10^4}{T^3} \quad (14)$$

4.2 SAS4A/SASSYS-1 Model

The TSTF facility was modeled with SAS4A/SASSYS-1 Version 5.5.1. SAS4A/SASSYS-1 requires at least one core channel in a model. Because the TSTF benchmark specification does not provide information on the components of the facility except the test vessel, a small single-channel core model is utilized to fulfill the code's requirement of at least one core channel. Total reactor power is set to zero because the temperature and flow boundary conditions of sodium flowing into the test vessel are achieved via the PRIMAR-4 heat transport system model. Key geometry parameters for the core model, which were determined to ensure the appropriate boundary conditions into the test vessel, are listed in Table II.

Table II Key parameters for the core model of the SAS4A/SASSYS-1 TSTF model

Parameters	Values
Axial length of lower reflector	0.1 m
Axial length of fuel	0.4 m
Axial length of gas plenum	1.0E-5 m
Axial length of upper reflector	0.062 m
Cladding outer/inner radius	3.48E-3 / 4.0E-3 m
Thickness of outer/inner reflector nodes	1.0E-6 m

The PRIMAR-4 heat transport system model of SAS4A/SASSYS-1 models ex-core heat transport systems. Compressible volumes (CV#) are zero-dimensional volumes used to model large volumes such as inlet and outlet plena and pools. CVs are connected by liquid segments (S#), which consist of one or more elements (E#) representing one-dimensional, incompressible, and single-phase flow and are used to model pumps, pipes, valves, heat exchangers, steam generators, and more [5]. By default, SAS4A/SASSYS-1 employs a perfect mixing model to calculate the liquid temperature of a CV with a single representative temperature. In addition to the perfect mixing model, a stratified volume model is available. The stratified volume model can be activated with additional input parameters such as the configuration of the inlet to the stratified volume, the core radius, the minimum temperature difference for switching between stratified stages, the entrainment length, and more.

Figure 5 illustrates the TSTF PRIMAR-4 model. CV2 is the test vessel, represented as an outlet plenum CV with cover gas. The TSTF experiments were simulated with CV2 represented with both the perfect mixing and stratified volume models. CV1 represents the inlet plenum supplying sodium to the core model, and CV3 represents an incompressible liquid volume upstream of the core. Segment 1, which connects CV1 and CV2, includes the core element, Element 1. Segment 2 connects CV2 and CV3 and includes hot leg piping and an intermediate heat exchanger (IHX) component used to achieve the transient boundary condition for the test section inlet temperature. The test supply reservoir is represented using the simple IHX model with a table of primary side outlet temperatures as a function of time. Segment 3 connects CV3 and CV1 and includes cold leg piping and a pump element used to achieve the transient boundary condition for the mass flow rate into the test section. The pump is modeled using the simple tabular pump model with a table of relative pump head as a function of time. The test vessel inlet temperature and flow rate during the transient were specified to match the TSTF measured data for each test. To simulate the rapid decrease of the flow rate by the trip of the pump at the end of each test, the orifice coefficient at the bottom of the lower reflector zone was set to a value of 300 based on a sensitivity calculation designed to determine sufficient hydraulic losses that will achieve the lowest flow rates during the tests.

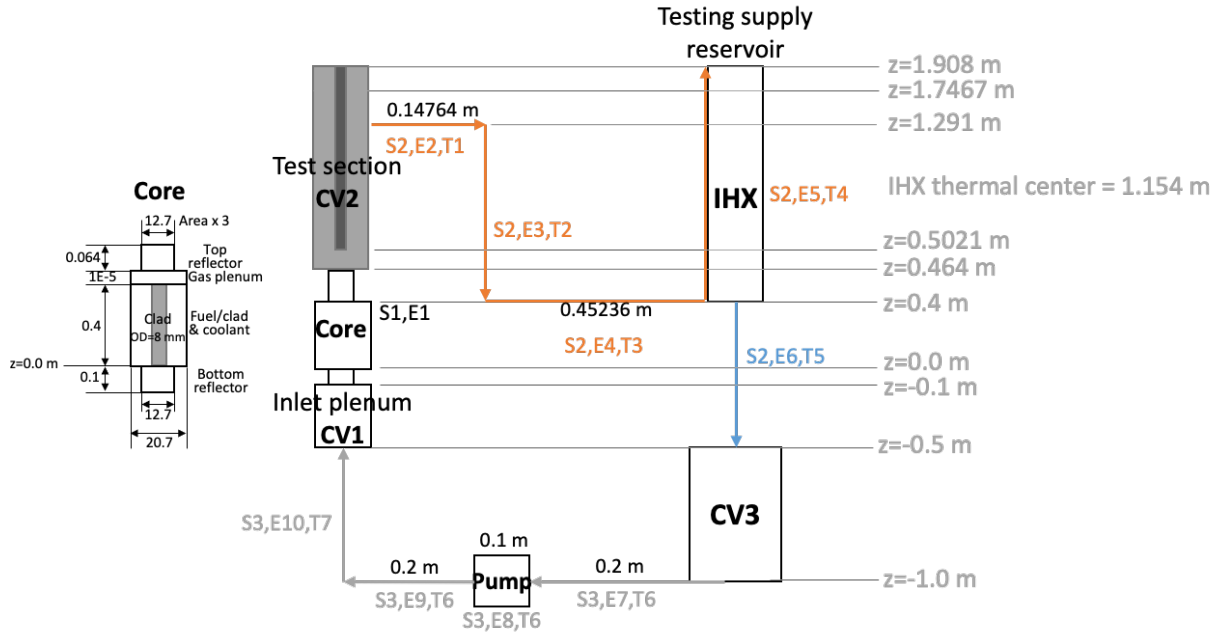


Figure 5 The TSTF PRIMAR-4 model

Table III summarizes key inputs for the TSTF PRIMAR-4 components. Because the TSTF benchmark specification does not provide the dimensions for components other than the test vessel, the dimensions of CV1 and CV3 and the elements in the 3 segments were approximated. The selected geometric inputs for those components were verified to preserve the transient flow and test vessel inlet temperature boundary conditions set by the pump and heat exchanger components.

Table III TSTF PRIMAR-4 model components

S#	E#	Type	Flow area [m ²]	Hydraulic diameter [m]	Length [m]	Bends Count [-]
1	1	Core	3.8003E-4	1.2700E-2	0.564	0
2	2	Pipe	1.9793E-4	1.5875E-2	0.14764	0
	3	Pipe	1.9793E-4	1.5875E-2	0.891	0
	4	Pipe	1.9793E-4	1.5875E-2	1.96036	1
	5	IHX	1.9793E-4	1.5875E-2	1.508	0
	6	Pipe	5.0671E-4	2.5400E-2	0.9	0
3	7	Pipe	5.0671E-4	2.5400E-2	0.2	0
	8	Pump	5.0671E-4	2.5400E-2	0.1	0
	9	Pipe	5.0671E-4	2.5400E-2	0.2	0
	10	Pipe	5.0671E-4	2.5400E-2	0.5	0

4.2.1 Parametric Sensitivity of Stratified Volume Model of SAS4A/SASSYS-1

In addition to the parameters related to the test conditions and geometries, users are able to define model parameters for the stratified volume model of SAS4A/SASSYS-1 such as the entrainment length and the minimum temperature difference for switching between stratified stages. The value of entrainment length (XLENTN) is used in calculating an entrainment rate of a hot plume. The minimum temperature difference for switching stages (EPSTST) is used to determine the formation and collapse of layers relative to the temperature of the incoming jet. When the temperature difference between adjacent stratified layers decreases below the value of EPSTST, a transition between stratification stages is possible. In addition to these modeling parameters, the user may define the orientation of the inlet to the stratified volume, either vertical or horizontal, depending on the incoming jet trajectory.

Figure 6 shows a comparison of the temperature evolution inside the test vessel for various input values of XLENTN and EPSTST for no UIS (Exp129 and Exp133) where the row indicates EPSTST values of 0.1, 1.0, and 10.0 from the left, and the column indicates XLENTN values of 0.01, 0.1, 1.0, 10.0, and 100.0 from the top. For Exp129, the layer temperature evolution became slower in the initial phase as the value of EPSTST increased. As a larger EPSTST delays stratified layer development and allows a larger temperature difference between adjacent layers at the initial phase of the test, and vice versa, it also accelerates the collapse of stratified layers in the later phase of the test with a smaller temperature difference between layers. The temperature distribution in the test vessel was observed to be insensitive to XLENTN for this series of experiments. Given that all TSTF tests were conducted by injecting a colder plume flowing into a hotter pool, no significant impact on the axial temperature results was expected. For Exp133, the two parameters showed trends similar to those of the low flow rate case.

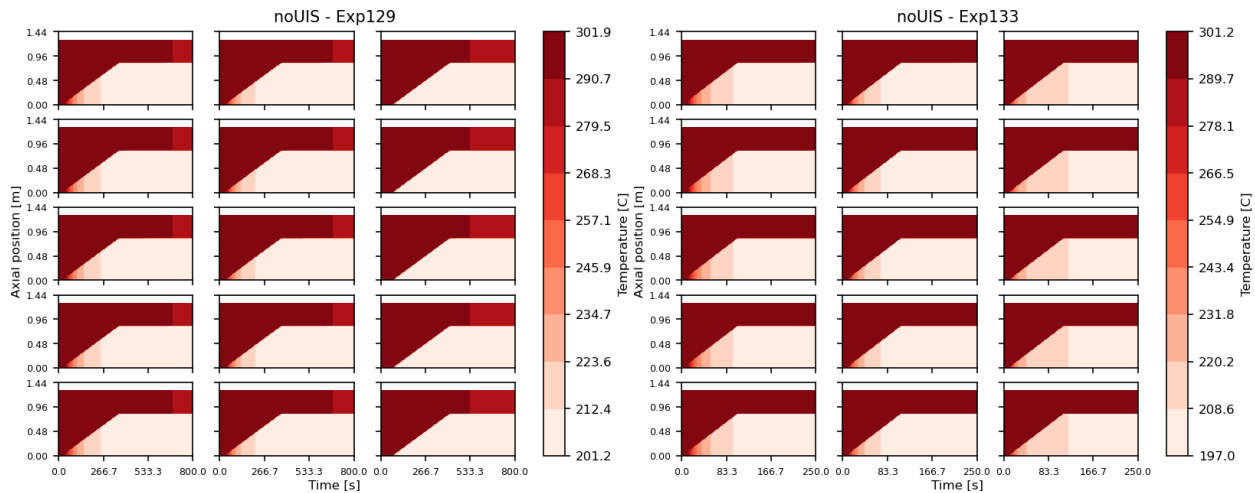


Figure 6 Parametric sensitivities of no UIS cases with respect to XLENTN and EPSTST

Figure 7 shows a comparison of the temperature evolution inside the test vessel for various input values of XLENTN, EPSTST, and inlet orientation for a solid UIS (Exp224 and Exp227). For the solid UIS cases, the UIS is located above the inlet channels with a small distance between the inlet and bottom of the UIS, and the incoming jet is expected to hit the structure first and disperse in a radial direction, which cannot be accounted for in the SAS4A/SASSYS-1 model with a crude 1-D geometrical representation of the test vessel. To determine a better representation of

the solid UIS cases, a horizontal inlet orientation was compared with the results of the vertical inlet orientation, in addition to varying the XLENTR and EPSTST parameters. For Exp224 with a vertical inlet option, the stratified layers were not predicted with a small EPSTST. With a horizontal option, all tests showed the stratified volume layers and their evolutions. The reason for this discrepancy is unknown and requires additional investigation. Additionally, with the horizontal option, a large value of EPSTST was observed to cause the unintentional collapse of the layer, shown near ~ 300 s, and requires further investigation. Similar to the cases without a UIS, the XLENTR values do not impact the temperature distributions. For Exp227 with the vertical inlet option, stratified volume layers were not observed with a low value for XLENTR; however, stratified layers formed for larger value of XLENTR as it depressed hot fluid entrainment at the layer interface. With a horizontal inlet option, stratified volume layers were predicted with all ranges of XLENTR and EPSTST. Based on these results, $XLENTR = 1.0$ and $EPSTST = 2.0$ were chosen for all TSTF simulations in this work, and a horizontal inlet option was set for the solid UIS and variable UIS cases to better describe the actual condition of the test vessel.

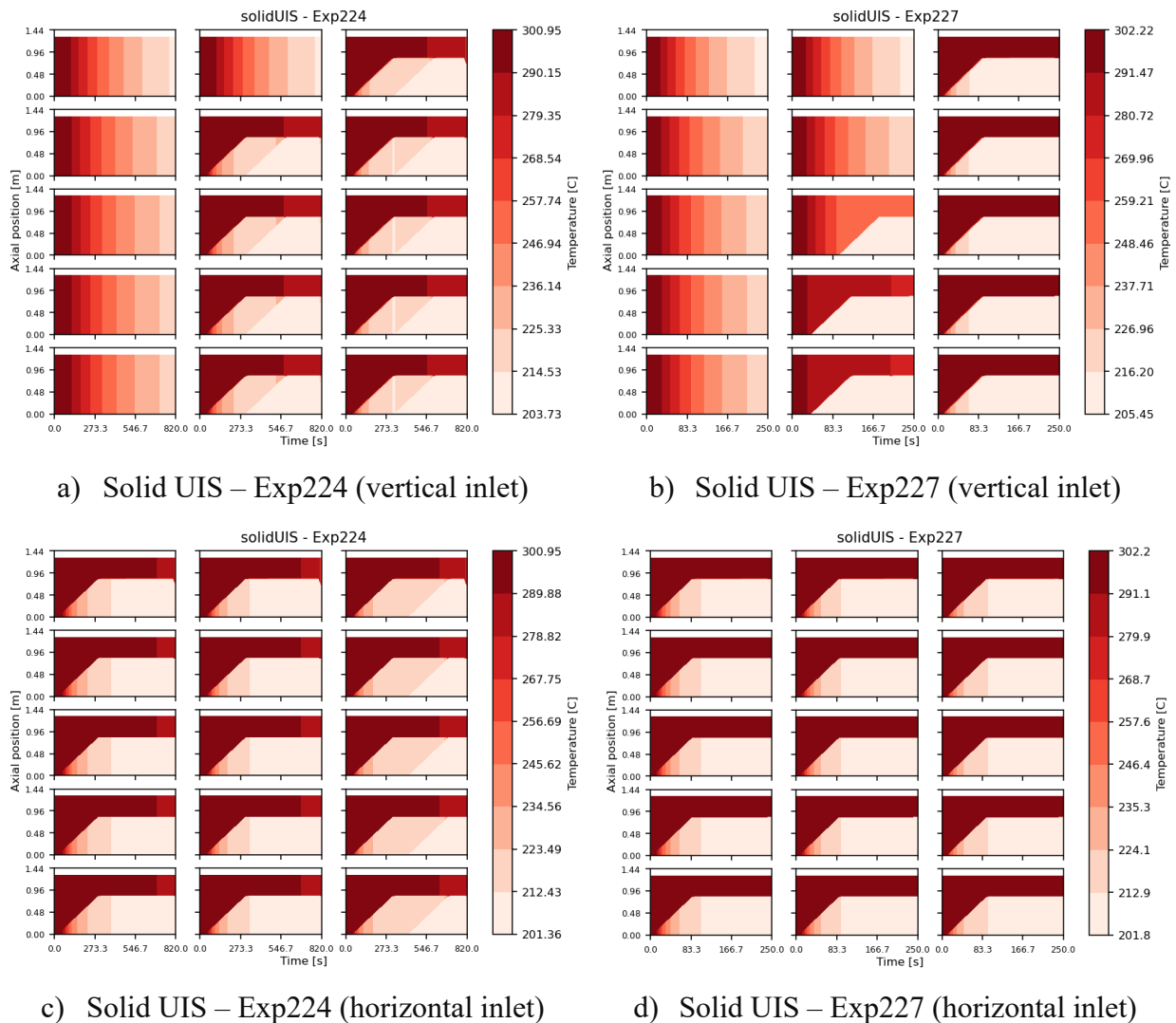


Figure 7 Parametric sensitivities of solid UIS cases with respect to XLENTR, EPSTST, and inlet orientation

Table IV. Test matrix for parametric sensitivity of the 1-D axial mixing model of SAM

	Modeling approaches	C_{gb}	C_{gv}	
			No UIS	Solid UIS
No mixing	1-D without axial mixing model	-	-	-
Ref	1-D axial mixing model	1.0	2.4738E-2	3.9920E-1
Case 1		0.0	2.4738E-2	3.9920E-1
Case 2		0.0	2.4738E-1	3.9920E+0
Case 3		1.0	0.0	0.0
Case 4		10.0	0.0	0.0

Figure 9 shows the comparison of the sodium temperature in the test vessel at various axial locations by varying parameters C_{gb} and C_{gv} of the 1-D axial mixing model of SAM for the no UIS cases. A larger velocity coefficient causes the temperature drop to occur earlier by promoting the mixing effect without the buoyancy effects with $C_{gb}=0$ (Case 1 and 2). The buoyancy coefficient itself tends not to be sensitive to mixing without the velocity effects with $C_{gv}=0$ (Case 3 and 4). Regardless of flow rate, noticeable differences with and without mixing effects in the test vessel were not observed in all locations.

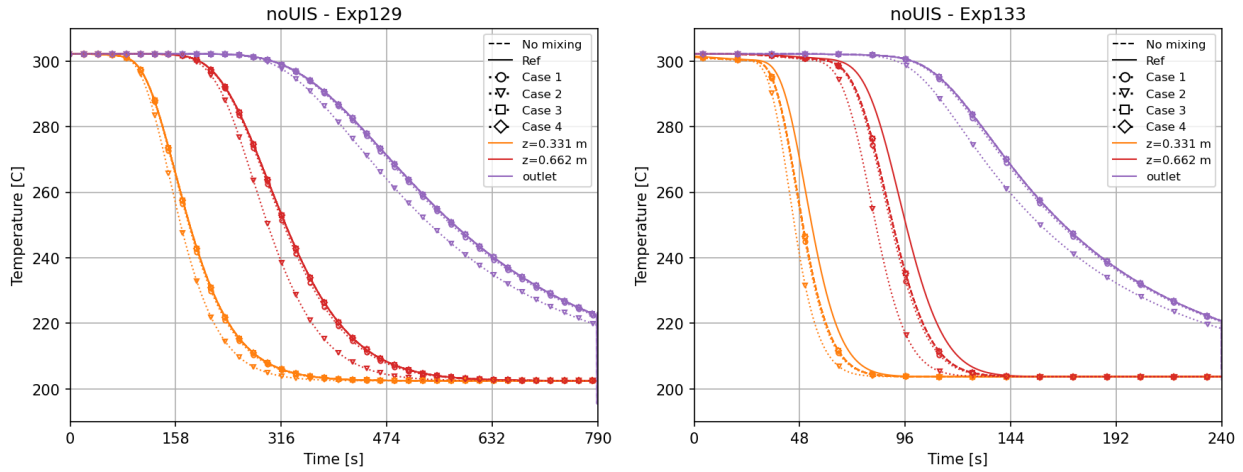


Figure 9 Parametric sensitivity of the 1-D axial mixing model of SAM – no UIS cases

Figure 10 shows the comparison of the sodium temperature in the test vessel at various axial locations by varying parameters C_{gb} and C_{gv} of the 1-D axial mixing model of SAM for the solid UIS cases. As shown in the cases without an UIS, a larger velocity coefficient (C_{gv}) incurred an earlier drop in temperature at all locations as it promotes mixing in cases without buoyancy effects with $C_{gb}=0.0$ (Case 1 and 2), where the difference between two cases were larger due to smaller volume of the test vessel than those of UIS cases. Similar to the cases without an UIS, no noticeable changes were made with varying the buoyancy coefficients (C_{gb}) without velocity effects with $C_{gv}=0.0$ (Case 3 and 4). In the TSTF test operation conditions and geometries, these two coefficients showed relatively little impact in predicting temperature distributions. Therefore, the default values of C_{gb} and C_{gv} of 1.0 and half of the inlet area ratio of the TSTF, i.e. 2.4738E-2 for no UIS cases and 3.9920E-1 for solid UIS cases, were used for all TSTF benchmark simulations using the 1-D axial mixing model of SAM.

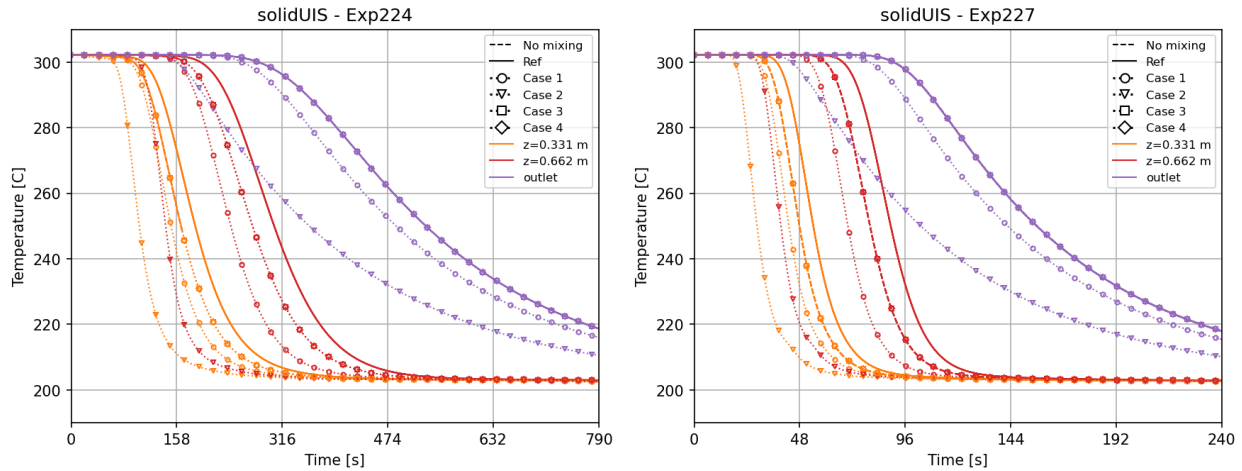
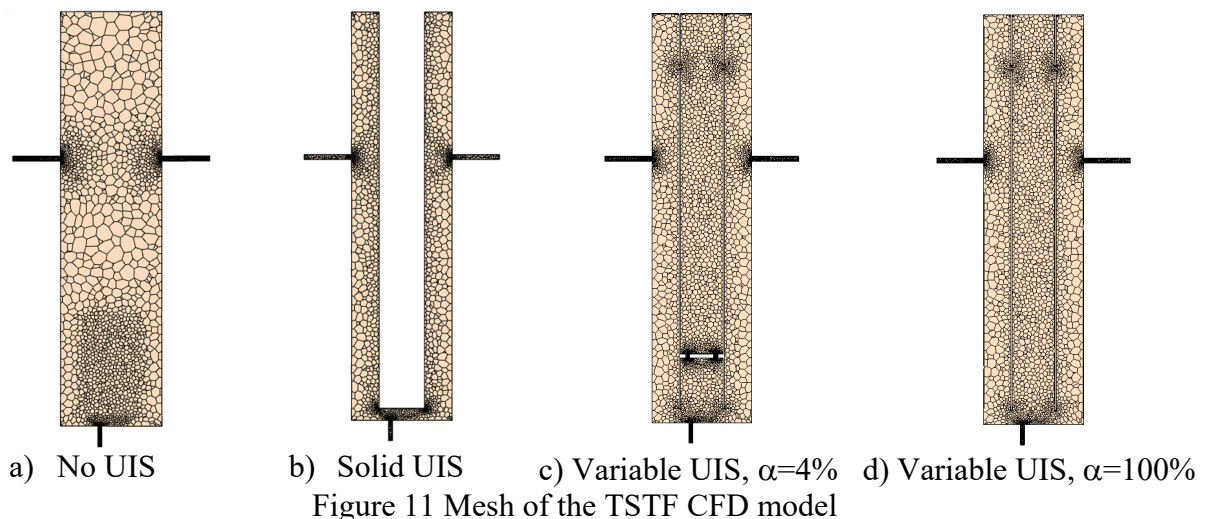


Figure 10 Parametric sensitivity of the 1-D axial mixing model of SAM – solid UIS cases

4.4 CFD Model

The URANS-based simulation of the test vessel was performed using the commercial CFD code, STAR-CCM+ v2022.01 [8]. The computational domain is simplified from the full geometry of the test vessel. A uniform inlet profile is used for both temperature and velocity at the three inlets interpolated directly from the experimental measurements, and the two outlets are set as pressure outlets. Solid structures including the vessel, the UIS, and the orifice plate for variable UIS cases are excluded to minimize computational costs, and all wall surfaces are set as adiabatic boundary conditions. Cover gas at the top of the test vessel is not considered, and the top wall of the test vessel is set as a no-slip wall condition. The computational meshes utilized are shown in Figure 11, where a two-layer all y^+ near-wall treatment is adopted with polyhedral mesh, and local mesh refinement on the region of highest gradients is applied at the bottom of the test vessel and the interface area between the test vessel and outlet pipes. Starting with the test vessel temperature initially uniform, full transients of each test are simulated by URANS with a realizable k-epsilon turbulence model. As the present work focused on the assessment of the model of each software in different fidelities, sensitivity on the turbulence model was not conducted. Discussions on the URANS turbulence models are included in Section 5.2.



5 Results and Discussions

5.1 TSTF Benchmark Results

Figure 12 to Figure 15 show comparisons of temperature distribution in the test vessel of the TSTF benchmark using the perfect mixing model and the stratified volume model of SAS4A/SASSYS-1 for no UIS, solid UIS, and variable UIS cases, respectively. For most of the test sets, a significant temperature gradient and thermal stratification phenomena were observed except for two cases with a high flow rate: Exp133 with no UIS and Exp283 with the variable UIS and 100 % internal flow area. For Exp133 and Exp283, a single-point sodium temperature within the test vessel as a function of time calculated by the perfect mixing model well represents the overall sodium temperature inside the test vessel due to the high injection rate, which promoted mixing in the test vessel. Beyond these conditions, the perfect mixing model does not predict the sodium temperature evolution within the test section well.

The stratified volume model of SAS4A/SASSYS-1 calculates representative temperatures of each layer (up to 3) and the evolution of the stratified layers over time. It showed the capability to predict the movement of the layer interface and hotter sodium temperatures in the region above the outlet. Although no significant stratification was observed for the no UIS with a high flow rate case (Exp133) except for the region above the outlet (at $z=0.864$ m), the results showed that the stratified volume model may overpredict thermal stratification phenomena in certain conditions such as a cylinder with a high L/D ratio and a small area jet flowing into a pool, like the TSTF test vessel. This may be due to the calculation method being based on existing correlations developed for a large plenum with a free jet.

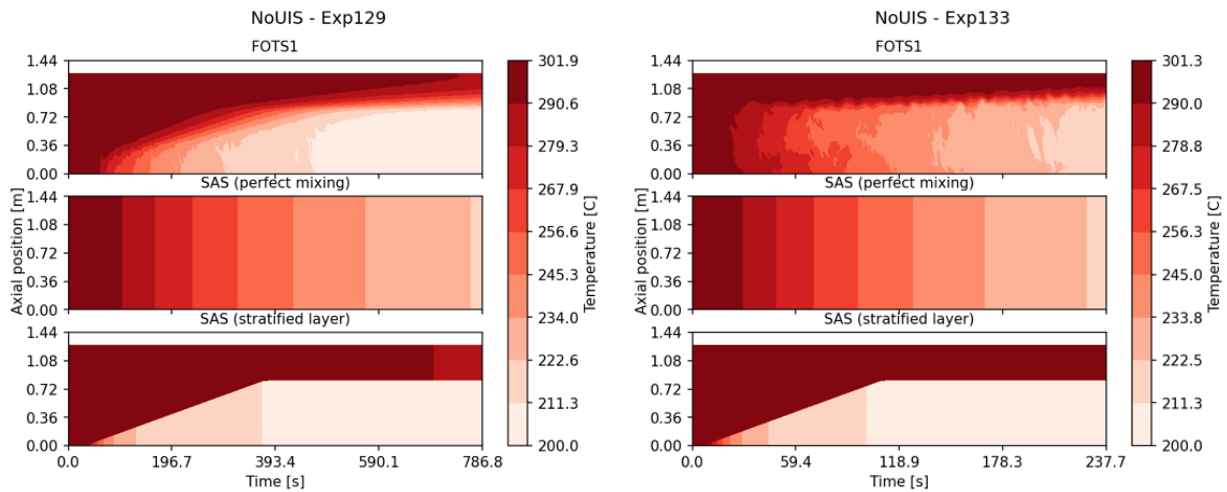


Figure 12 Temperature distribution in the test vessel using SAS4A/SASSYS-1 – No UIS cases

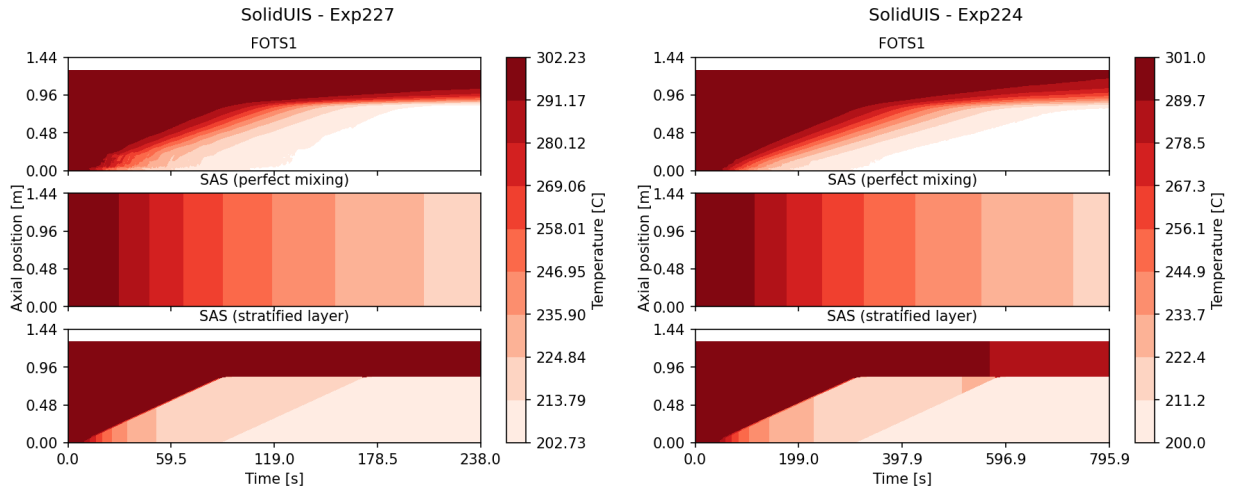


Figure 13 Temperature distribution in the test vessel using SAS4A/SASSYS-1 – Solid UIS cases

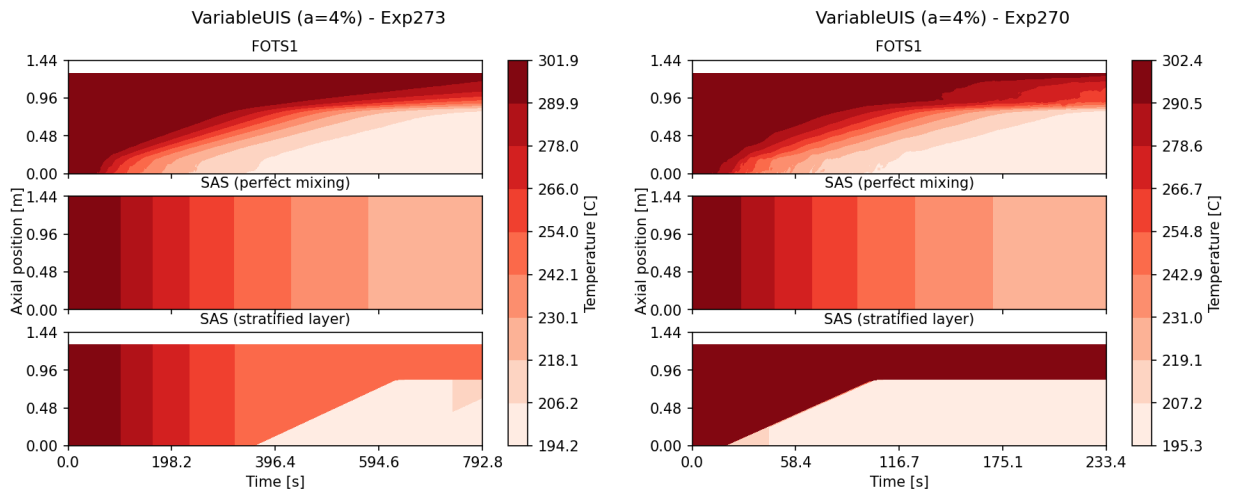


Figure 14 Temperature distribution in the test vessel using SAS4A/SASSYS-1 – Variable UIS, $\alpha=4\%$ cases

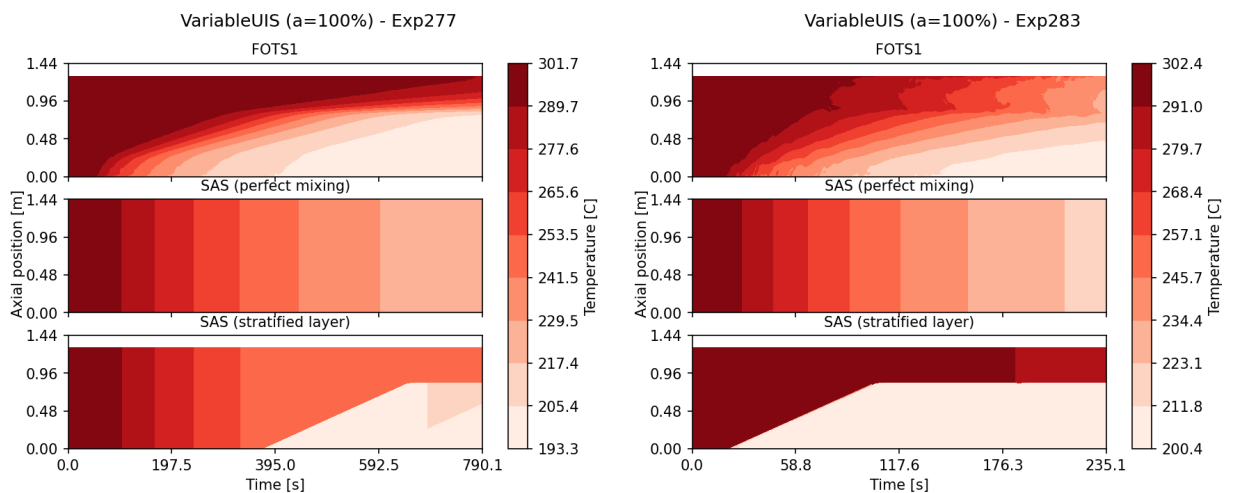


Figure 15 Temperature distribution in the test vessel using SAS4A/SASSYS-1 – Variable UIS, $\alpha=100\%$ cases

Figure 16 to Figure 19 show quantitative comparisons of the local sodium temperatures in the test vessel of the TSTF benchmark using the perfect mixing model and the stratified volume model of SAS4A/SASSYS-1 for no UIS, solid UIS, and variable UIS cases, respectively. For the cases where stratified layers were predicted, rapid increases and decreases of the sodium temperatures were predicted by the stratified volume model of SAS4A/SASSYS-1 for most of the cases. This was caused by the shift of the thermal layer as the thermal stratification stage propagates upwards, where the entire test vessel is represented with at most three temperature layers. Because the influence of internal flow through the UIS was not fully incorporated into the model, the stratified volume model of SAS4A/SASSYS-1 showed poor performance in predicting local temperature distributions and the time evolution.

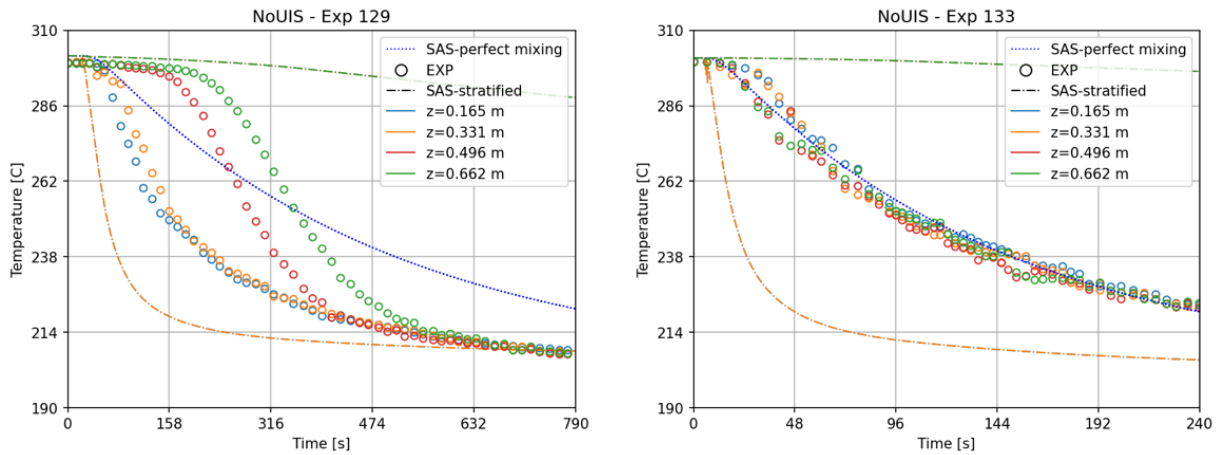


Figure 16 Comparison of sodium temperature distribution in the test vessel (SAS4A/SASSYS-1) – no UIS cases

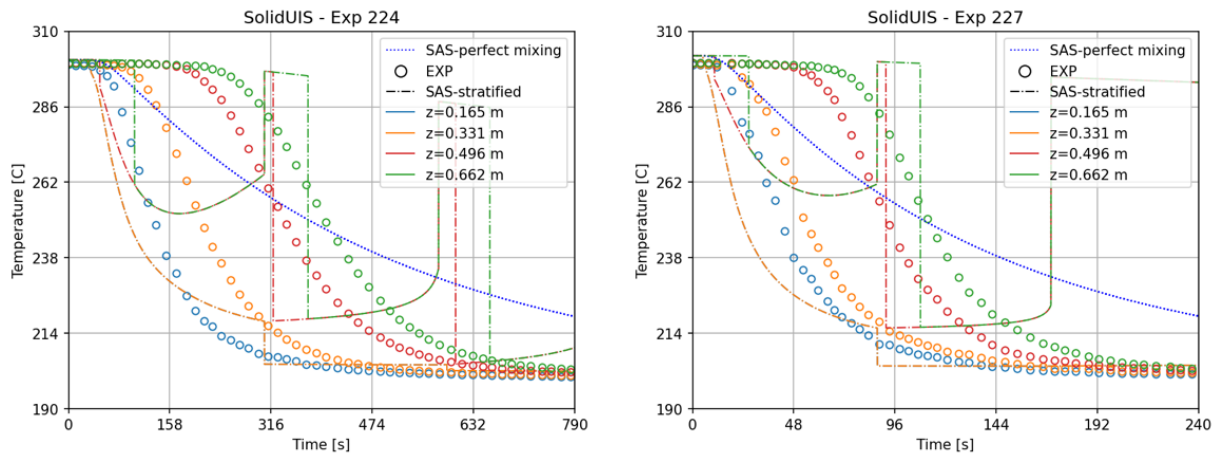


Figure 17 Comparison of sodium temperature distribution in the test vessel (SAS4A/SASSYS-1) – Solid UIS cases

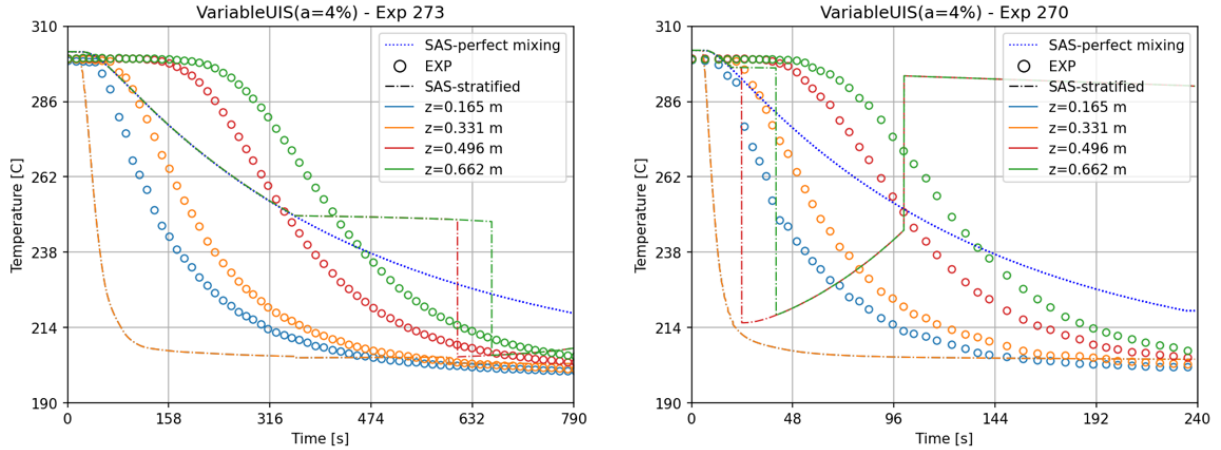


Figure 18 Comparison of sodium temperature distribution in the test vessel (SAS4A/SASSYS-1) – Variable UIS, $\alpha=4\%$ cases

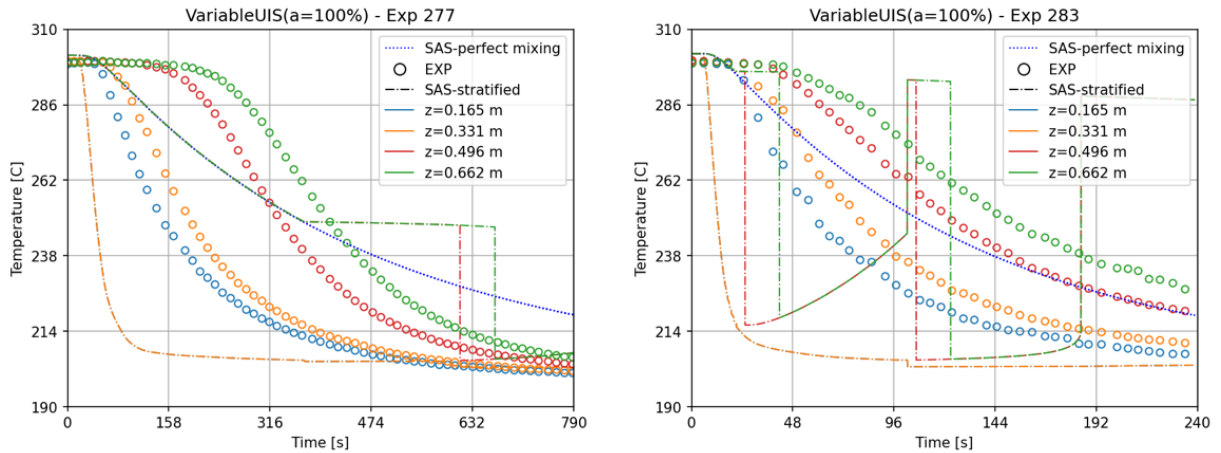


Figure 19 Comparison of sodium temperature distribution in the test vessel (SAS4A/SASSYS-1) – Variable UIS, $\alpha=100\%$ cases

Figure 20 to Figure 23 show comparisons of the sodium temperature in the test vessel of the TSTF benchmark tests using SAM for no UIS, solid UIS, and variable UIS - $\alpha=4\%$ and $\alpha=100\%$, respectively. The 1-D axial mixing model of SAM showed good performance in predicting temporal temperature variations compared to measured data for most of the cases, but also predicted accelerated timing and faster changes in temperature than the measured data. In addition, for Exp133 and Exp283 where the sodium in the test vessel was well mixed, it did not capture enhanced thermal mixing. The 1-D axial mixing model showed consistency in performance, in that larger deviations between the model's prediction and the measured data were observed in higher flow rate cases for all UIS configurations. In high flow rate cases, thermal mixing phenomena is governed more by momentum than buoyancy due to temperature differences between the cold jet and hot pool, explaining the error in the SAM model as it is based on thermal mixing principals. It can also be observed that the 1-D axial mixing model of SAM showed better performance in predicting temperature distributions in $\alpha=4\%$ cases than $\alpha=100\%$ cases for the variable UIS tests, as momentum-driven mixing is dominant.

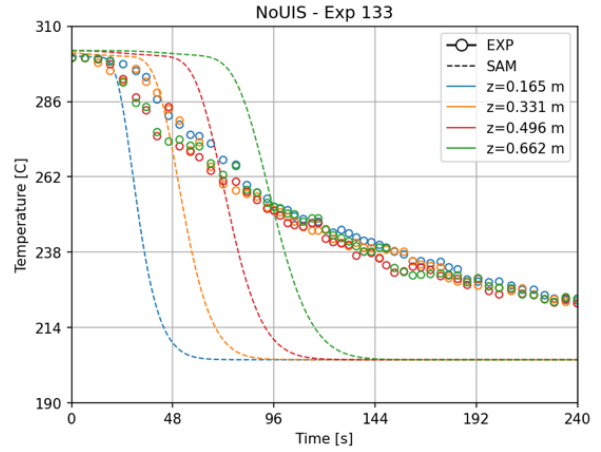
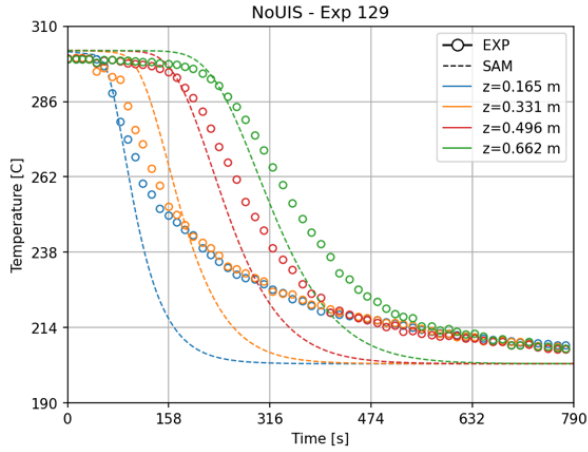


Figure 20 Comparison of temperature distribution in the test vessel (SAM) – no UIS cases

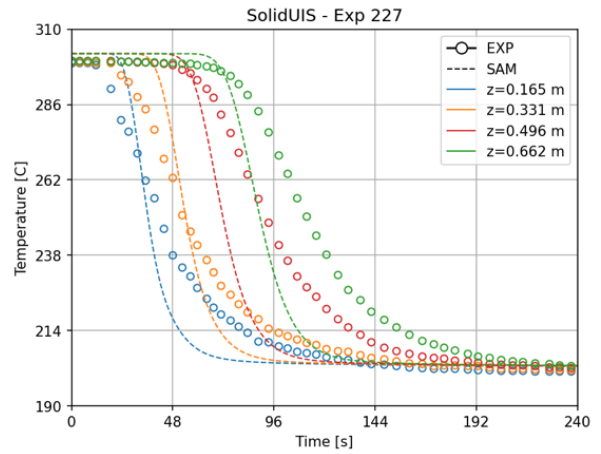
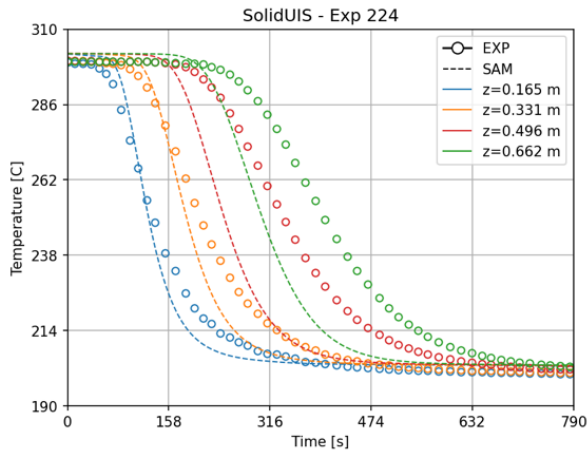


Figure 21 Comparison of temperature distribution in the test vessel (SAM) – solid UIS cases

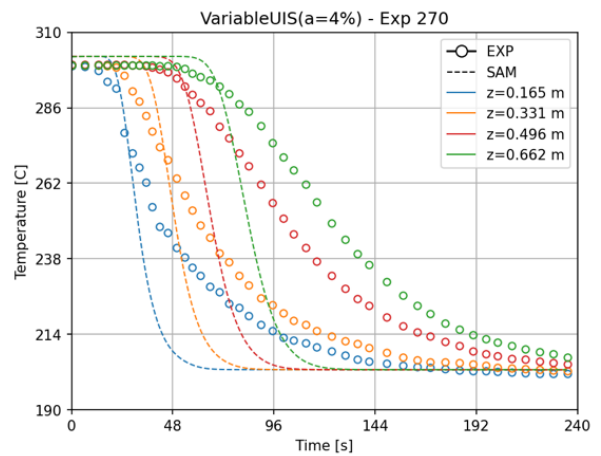
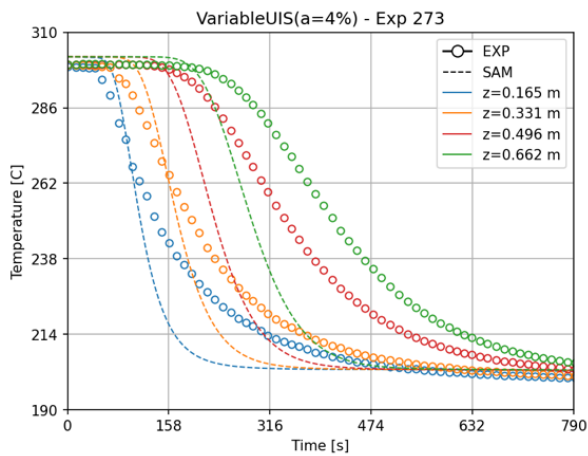


Figure 22 Comparison of temperature distribution in the test vessel (SAM) – variable UIS, $\alpha=4\%$ cases

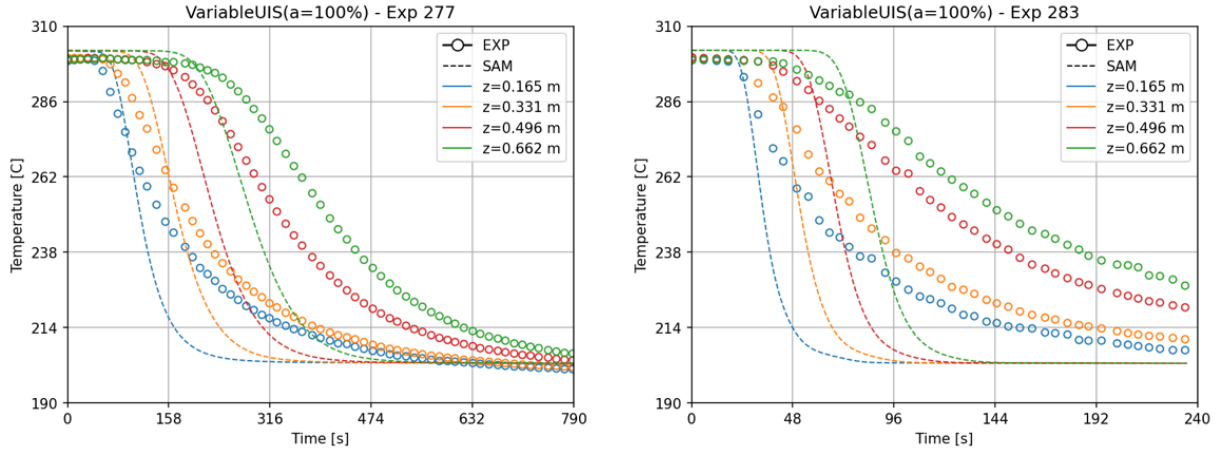


Figure 23 Comparison of temperature distribution in the test vessel (SAM) – variable UIS, $\alpha=100\%$ cases

Figure 24 to Figure 27 show comparisons of the sodium temperatures in the test vessel of the TSTF benchmark tests using CFD for no UIS, solid UIS, and variable UIS - $\alpha=4\%$ and $\alpha=100\%$, respectively. CFD results showed trends similar to the 1-D axial mixing model for prediction of temporal temperature variations, where both predicted accelerated timing and faster changes in temperature compared to the measured data. For the high flow rate case with solid UIS (Exp227), CFD predicted a temperature oscillation induced by local flow phenomena, but it was not observed in the actual experiment. This is strongly dependent on the level (or scale) of turbulence in turbulence models. This modeling artifact indicates that caution is necessary in using URANS results in real applications as they are highly dependent on turbulence modeling and the treatment considered. However, CFD showed good performance in predicting the temperature field of the variable UIS cases. Because the CFD model was able to include a detailed geometry of the UIS and its flow path, the influence of the internal flow through the UIS on the temperature field in the test vessel can be captured with CFD simulations. In the solid UIS case, all cold sodium entering the test vessel is radially dispersed out of the UIS and develops into a stratified layer that propagates toward the outlet. The variable UIS case allows the coldest sodium to enter the UIS and subsequently exit and propagate down to the outlets, resulting in increased thermal mixing in the test vessel as shown in Figure 28. With the aim of modeling geometries in detail, CFD can describe the influence of the internal flow through the UIS on the thermal field in the test vessel.

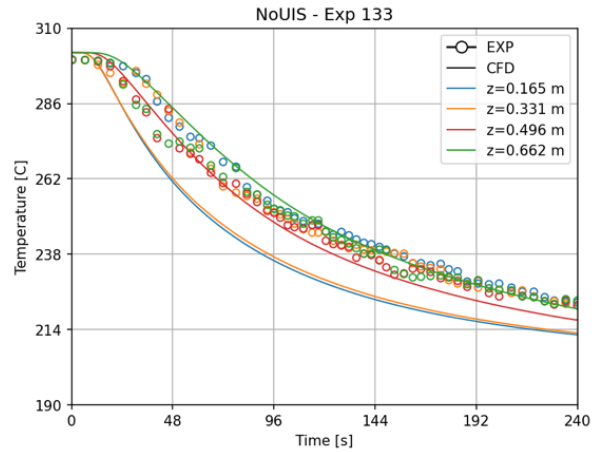
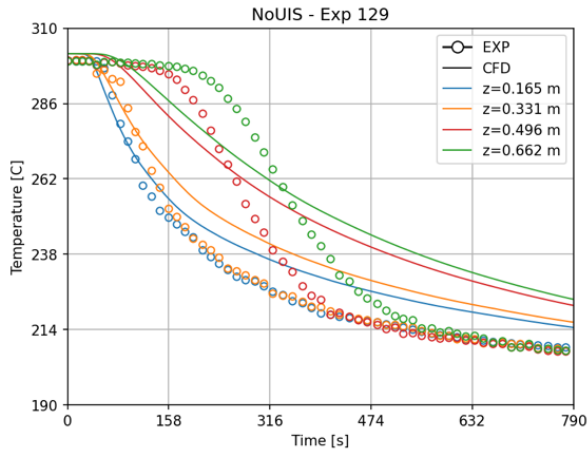


Figure 24 Comparison of temperature distribution in the test vessel (CFD) – no UIS cases

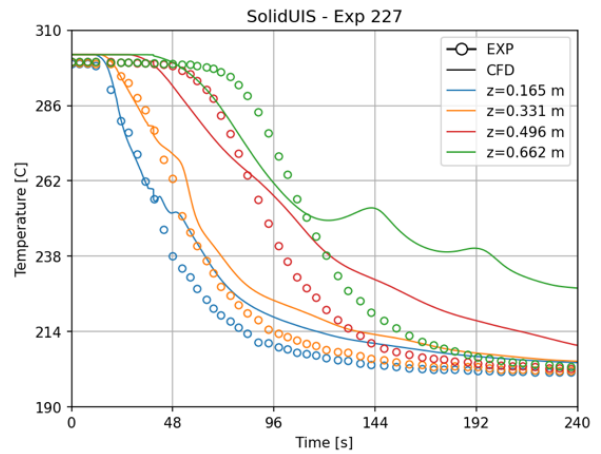
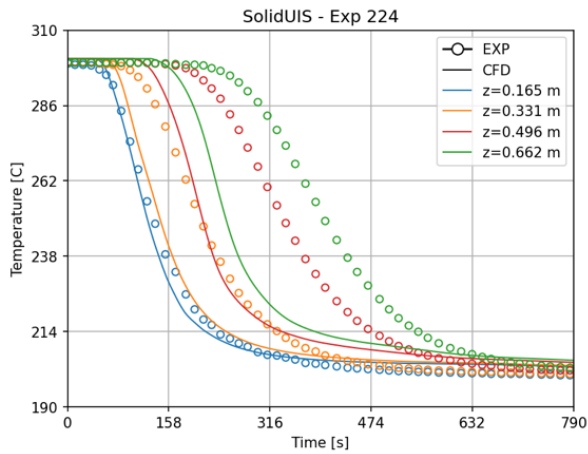


Figure 25 Comparison of temperature distribution in the test vessel (CFD) – solid UIS cases

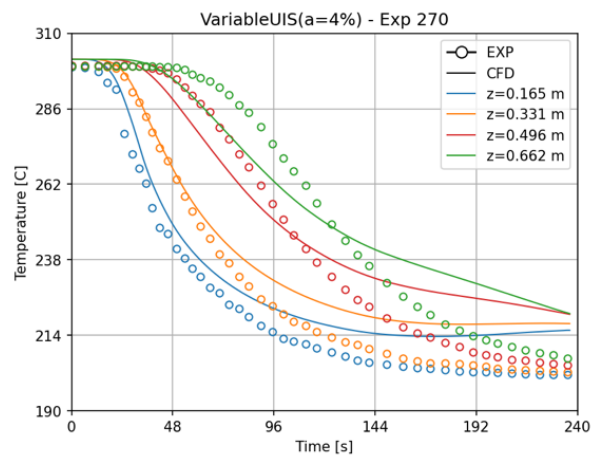
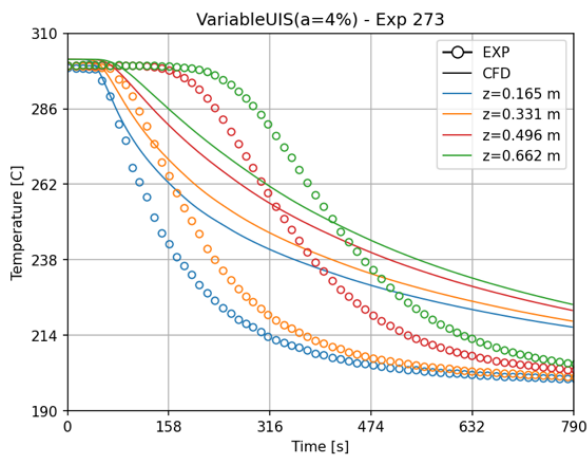


Figure 26 Comparison of temperature distribution in the test vessel (CFD) – variable UIS, $\alpha=4\%$ cases

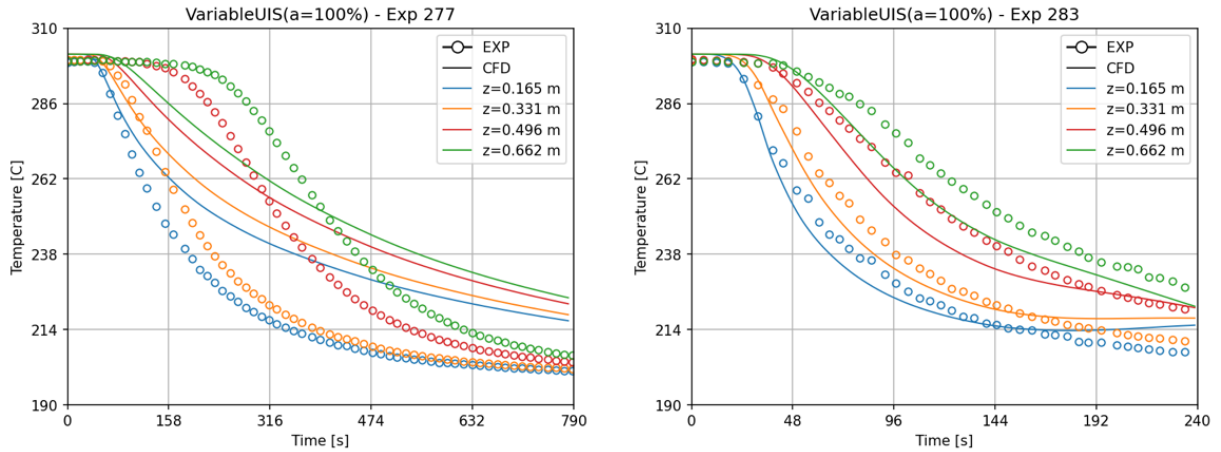


Figure 27 Comparison of temperature distribution in the test vessel (CFD) – variable UIS, $\alpha=100\%$ cases

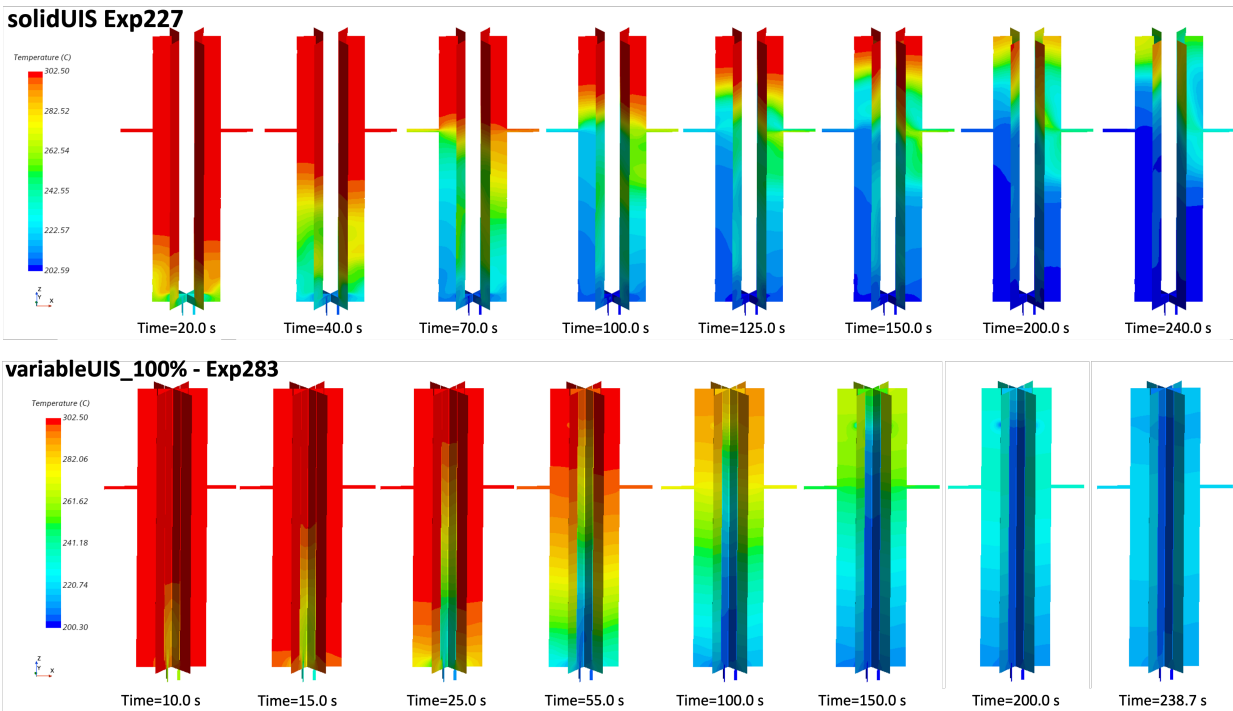


Figure 28 Snapshots of sodium temperature distribution in the test vessel using CFD.

Figure 29 shows the comparison of the TSTF test section outlet temperature with measured data and predicted results by each software for no UIS cases. For the no UIS low flow rate case (Exp129), prediction of the outlet temperature using the 1-D axial mixing model of SAM had a close trend with the experimental data with a minor delay of the temperature drop onset and rate. CFD predicted earlier timing for the onset of the temperature drop, but a lower slope of the outlet temperature drop. The stratified volume model of SAS4A/SASSYS-1 predicted the timing of temperature drop close to the measured data but had a rapid drop immediately. This is because the stratified layer interface positioned near the outlet moved upward and the outlet temperature is

then calculated from the colder lower stratified layer. For the no UIS high flow rate case (Exp133), the perfect mixing model of SAS4A/SASSYS-1 performed well in predicting outlet temperature trends. In this case, the test vessel sodium temperature can be represented as a single value as a high flow rate injection promotes thermal mixing of the sodium in the test vessel without any flow obstructions present. The 1-D axial mixing model of SAM and the stratified volume model of SAS4A/SASSYS-1 had large deviations from the measured data.

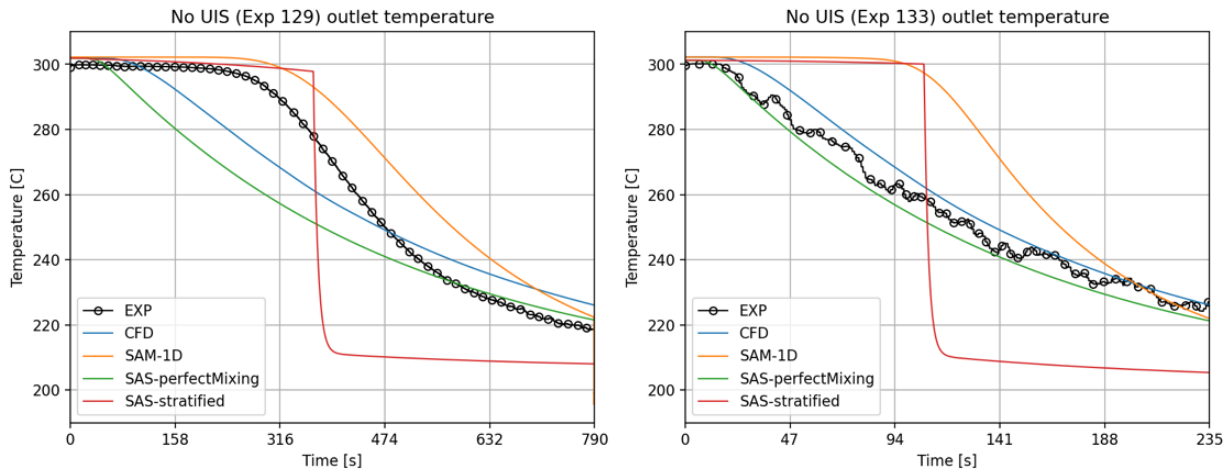


Figure 29 Comparisons of the test vessel outlet temperature results of TSTF benchmark – no UIS

Figure 30 shows the comparison of the TSTF test section outlet temperature with measured data and predicted results by each software for solid UIS cases. For the solid UIS cases (Exp224 and Exp227), the 1-D axial mixing model of SAM had good performance in predicting the timing and slope of the temperature drop of the experimental data. Because of the solid structures in the test vessel, the 1-D representation better describes the flow channel of the test vessel and the mixing phenomena. The stratified volume model of SAS4A/SASSYS-1 was able to predict outlet temperature drop time compared to the measured data, but had a large local deviation, especially with stepwise changes due to the shift of the stratified layer interface elevation and coarse representation of the test vessel temperature. CFD was able to predict the slope of the temperature drop but it had earlier timing of the onset of the temperature drop compared to the measured data. Even if the CFD model includes the UIS geometry, a complex flow pattern at the bottom of the test vessel made the overall temperature distribution asymmetric. As shown, the north and south outlet temperatures predicted by CFD were different from each other, while outlet temperatures for all experiments were measured at the branch where the two outlets are converging. The perfect mixing model of SAS4A/SASSYS-1 had poor performance in predicting outlet temperature trends for these tests.

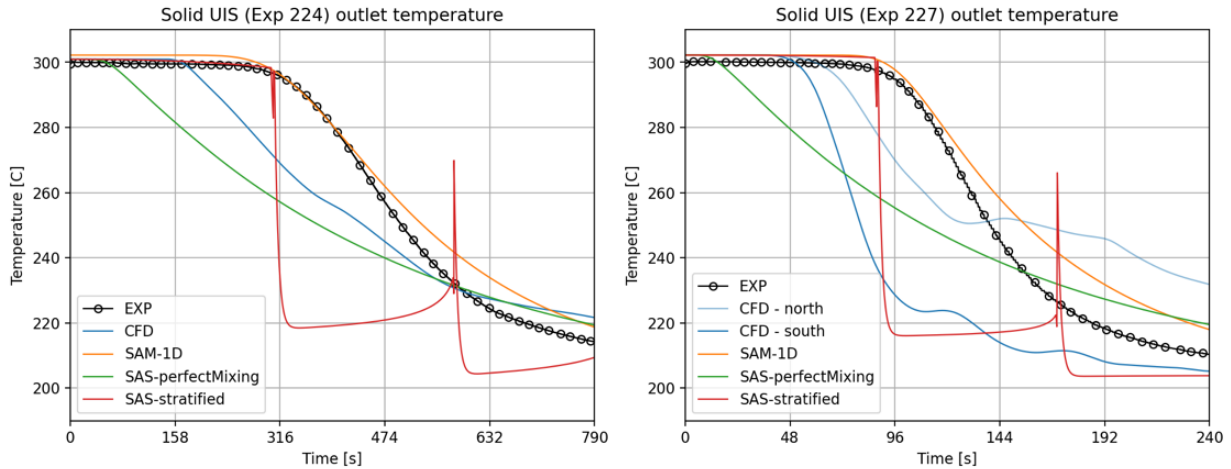


Figure 30 Comparisons of the test vessel outlet temperature results of TSTF benchmark – solid UIS

Figure 31 shows the comparison of the TSTF test section outlet temperature with measured data and predicted results by each software for variable UIS - $\alpha=4\%$ cases. For the variable UIS - $\alpha=4\%$ cases (Exp270 and Exp 273), the 1-D axial mixing model of SAM performed well, similar to the solid UIS cases. Even though flow through the UIS is not modeled in SAM, a small portion of the jet going into the UIS did not significantly impact the sodium temperature distribution. CFD showed better performance for these cases than the solid UIS cases, but its performance was dependent on the flow rate, having better performance in higher flow rate cases. It also showed fluctuations of velocity and temperature fields induced by flow obstructions including the UIS. The stratified volume model of SAS4A/SASSYS-1, which initially had no stratified layers, later developed stratified layers that predicted stepwise changes in outlet temperature caused by the shift of the interface near the outlets. The two models of SAS4A/SASSYS-1 had poor performance in the prediction of outlet temperature trends for these cases.

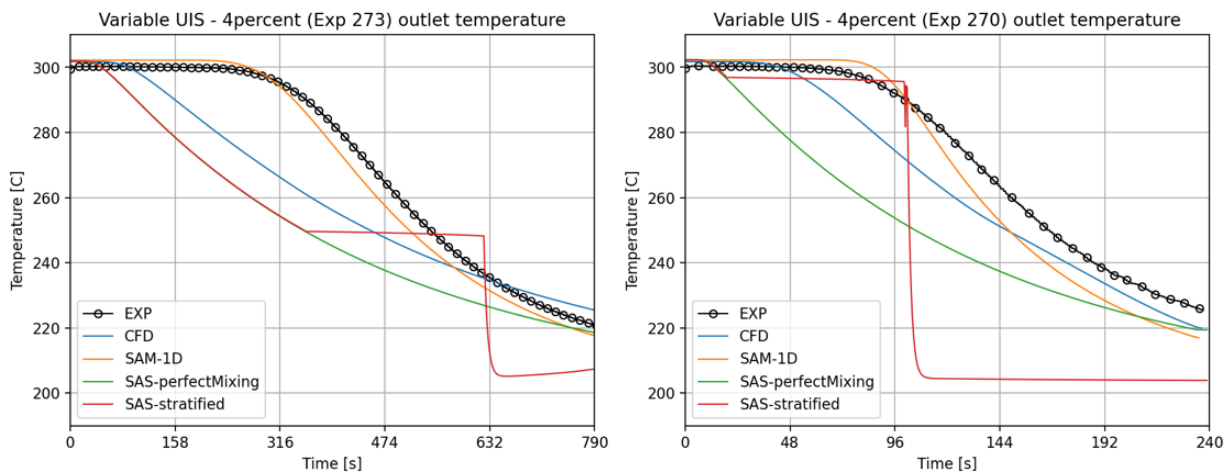


Figure 31 Comparisons of the test vessel outlet temperature results of TSTF benchmark – variable UIS, $\alpha=4\%$

Figure 32 shows the comparison of the TSTF test section outlet temperature with measured data and predicted results by each software for variable UIS - $\alpha=100\%$ cases. For the variable UIS - $\alpha=100\%$ cases (Exp277 and Exp283), the 1-D axial mixing model of SAM still performed well in predicting outlet temperature trends, especially for the low flow rate case (Exp277). Because the internal flow through UIS was not included in the SAM and SAS4A/SASSYS-1 models, both SAM and SAS4A/SASSYS-1 predicted outlet temperature trends that had large deviations from the measured data for the high flow rate case (Exp283). CFD predicted an earlier onset time and lower slope of temperature drop compared to the measured data in the low flow rate case but had better performance in the high flow rate case, as it models actual flow mixing with the top region of the test vessel by treatment of coolant flowing out of the UIS.

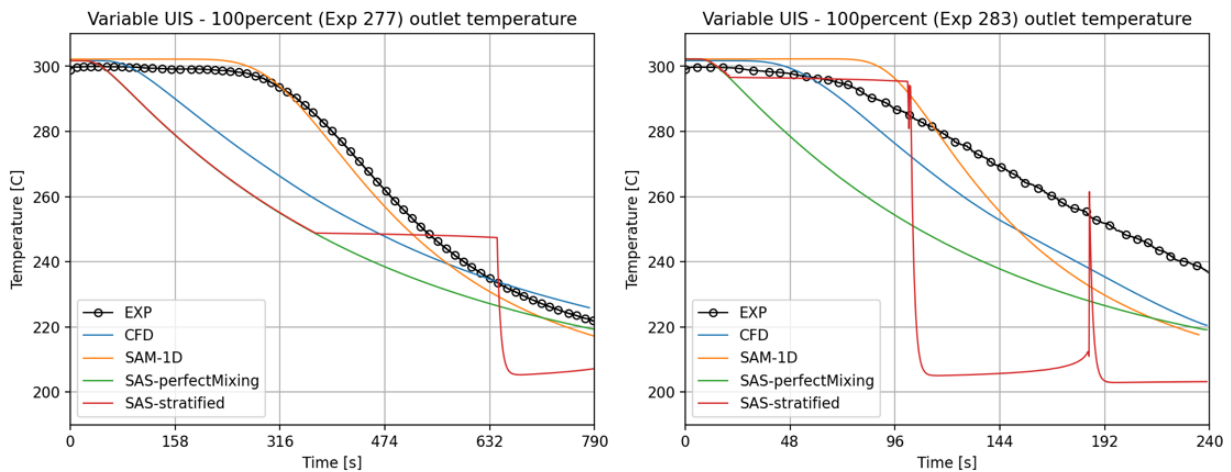


Figure 32 Comparisons of the test vessel outlet temperature results of TSTF benchmark – variable UIS, $\alpha=100\%$

In summary, the perfect mixing model of SAS4A/SASSYS-1 showed qualitatively good performance in predictions for high flow rates with no UIS (Exp133), as high flow rate injection promotes thermal mixing of sodium in the test vessel without flow obstructions. Other than this specific case, the perfect mixing model shows poor agreement with the measured data of both test vessel outlet temperature and the axial temperature distribution. The stratified volume model of SAS4A/SASSYS-1 is able to predict the delay of the outlet temperature drop in the low flow rate test of no UIS case (Exp129) and all solid UIS cases (Exp224 and Exp 227). Because the stratified volume model has a limited number of representative temperature layers, it shows rapid, nonphysical changes at certain times in all cases due to the formation and collapse of the stratified layers and moving interfaces near the outlet region. The 1-D axial mixing model of SAM showed good agreement with the measured data in the prediction of the temporal evolution of the sodium outlet temperature except for the case of high mixing without flow obstructions. Note that as the SAM and SAS4A/SASSYS-1 models did not simulate internal flow through the UIS, the deviations from the measured data of the variable UIS cases for the two computational models are mainly due to such modeling limitations. The 1-D axial mixing model of SAM shows the closest prediction to the measured outlet temperature for the four variable UIS cases. CFD results also show similar predictions as those of the 1-D axial mixing model of SAM in most cases. Because the CFD model treated the test vessel geometry in detail, it showed better performance in the

variable UIS cases by simulating internal flow through UIS and subsequent coolant mixing at the top of the test vessel.

To evaluate each model for the prediction of thermal stratification quantitatively, local deviations and the Root Mean Square (RMS) errors of the deviations are compared as defined in equation (15), where N_t is the number of total timesteps. As each time step of measured data and predicted results by the software may be different, experimental data was post-processed to maintain the same time steps as predicted results using linear interpolation, if necessary. Note that the results of the stratified volume model of SAS4A/SASSYS-1 were processed to compare temperature at local points by taking stratified layer temperature at certain elevations.

$$RMS = \sqrt{\sum_{i=1}^{N_t} (dev)^2 / N_t}, \text{ where } dev = [T_{measured} - T_{predicted}[^{\circ}C]] / T_{measured}[^{\circ}C] \quad (155)$$

Figure 33 to Figure 36 show local maximum and minimum deviations expressed as horizontal lines and time-averaged RMS errors of the computational results by comparison locations for no UIS, solid UIS, and variable UIS - $\alpha=4\%$ and $\alpha=100\%$, respectively. Most models had time-averaged RMS errors of less than 20% for all test cases except for the local points near the outlets of the stratified volume model of SAS4A/SASSYS-1. The large local deviations were a result of the stratified volume model of SAS4A/SASSYS-1, for which a representative stratified layer temperature close to the comparison point was utilized, as noted. Overall, CFD showed good performance with respect to minimum time-averaged RMS error as well as temporal deviations of the outlet temperature for all locations. The 1-D axial mixing model of SAM showed good performance with fairly small time-averaged RMS errors but had local deviations in outlet temperatures in cases of high flow rate with active mixing. The 1-D axial mixing model of SAM predicted temperatures in all locations at a level similar to those of CFD except for the variable UIS cases due to modeling limitations and constraints. Because the stratified volume model of SAS4A/SASSYS-1 had local, rapid step changes due to the transition of layers, it had large local errors at certain intervals. For cases with a higher flow rate without flow obstructions, the perfect mixing model of SAS4A/SASSYS-1 showed fair performance in the prediction of temperature distributions.

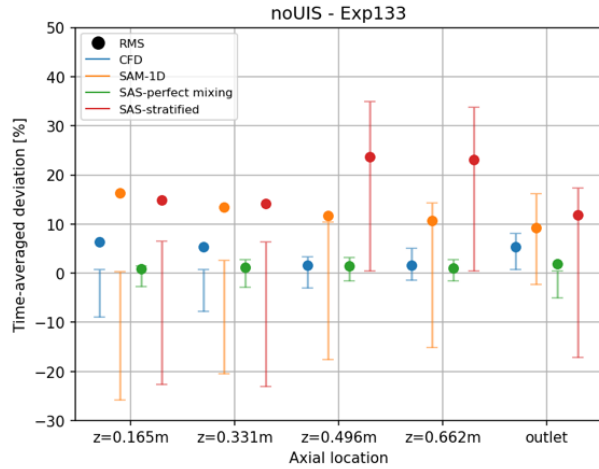
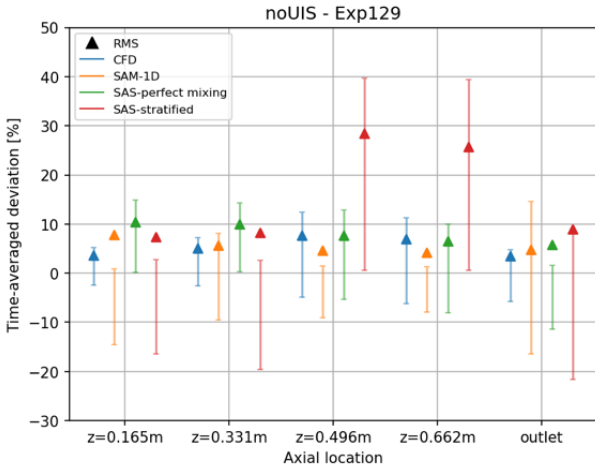


Figure 33 Time-averaged RMS error and local min/max deviations of no UIS cases

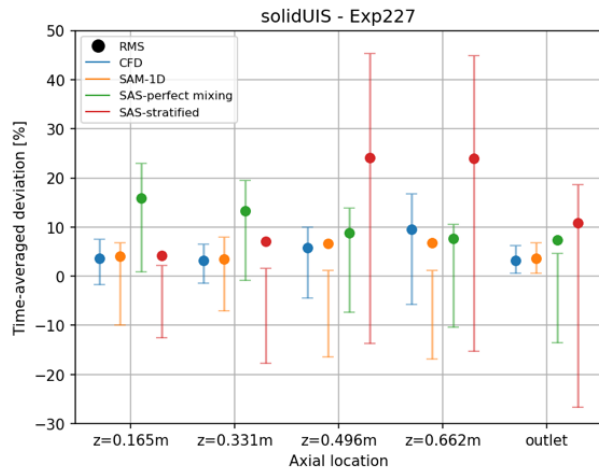
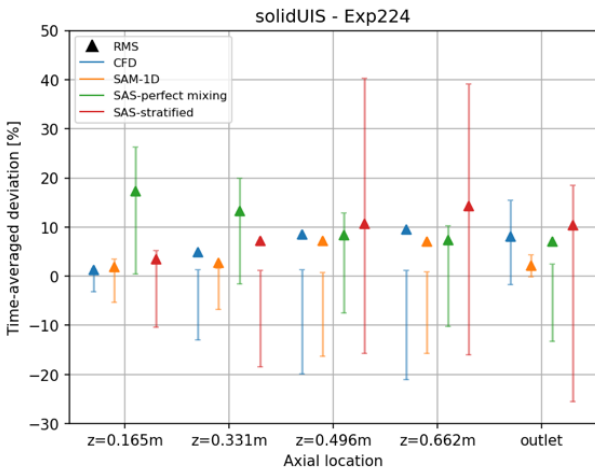


Figure 34 Time-averaged RMS error and local min/max deviations of solid UIS cases

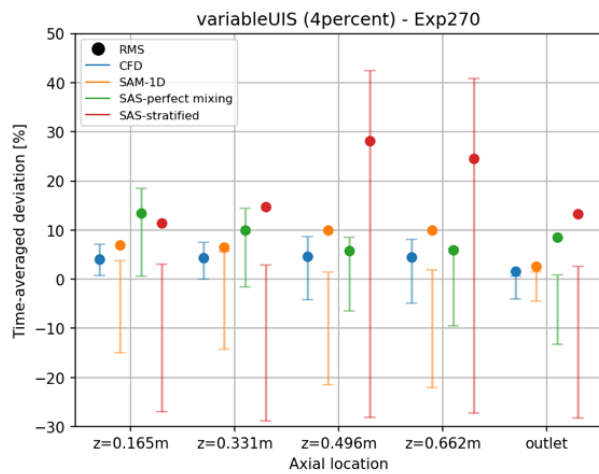
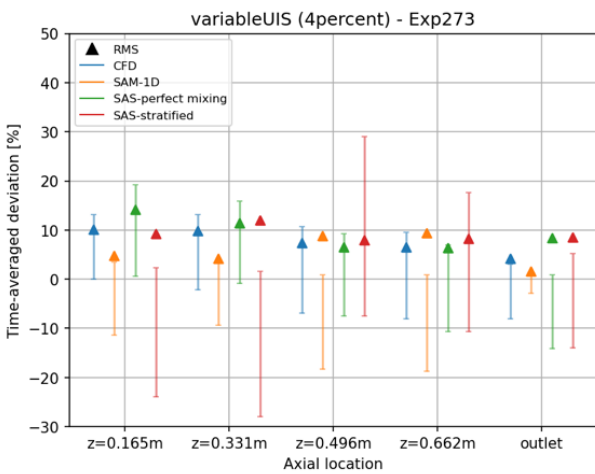


Figure 35 Time-averaged RMS error and local min/max deviations of various UIS, $\alpha=4\%$ cases

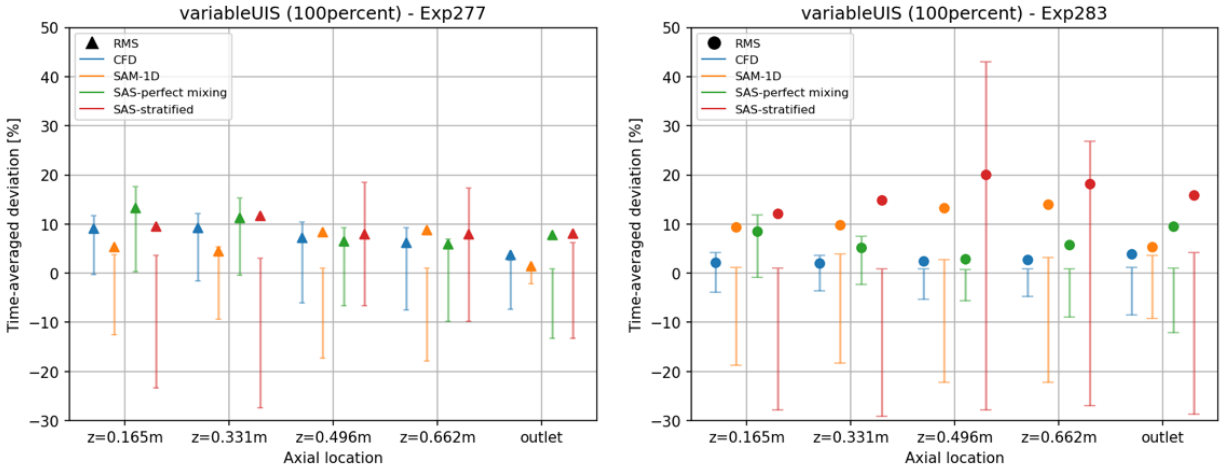


Figure 36 Time-averaged RMS error and local min/max deviations of various UIS, $\alpha=100\%$ cases

Table V attempts to summarize the performance of the thermal stratification models of each software in modeling of the TSTF benchmark tests. Qualitative grades have been assigned to each model for each of the tests. The following grades have been used:

- “Very good”: All temperature predictions compared showed a close match with the measured data.
- “Good”: Some of the temperature predictions showed a good match with the measured data.
- “Poor”: Prediction results did not capture the behavior of the outlet temperature evolution, or the quantitative comparisons of the temperature field were significantly different from the measured data.

For Exp129, the perfect mixing model of SAS4A/SASSYS-1 and CFD did not capture both the coolant temperature distribution and the outlet temperature evolution trends. The stratified volume model of SAS4A/SASSYS-1 predicted the time of the outlet temperature drop but did not characterize the temperature distribution of the test vessel sodium well. The 1-D axial mixing model of SAM showed good agreement in outlet sodium temperature evolution but had deviations in temperature distribution at the lower region of the test vessel.

For Exp133, the perfect mixing model of SAS4A/SASSYS-1 and CFD showed good performance in predicting both the sodium temperature distribution in the test vessel and the sodium outlet temperature evolution. The other two models showed similar trends in both temperature distribution in the test vessel and the outlet temperature.

For Exp224 and Exp227, the perfect mixing model of SAS4A/SASSYS-1 did not capture the thermal stratification phenomena. The stratified volume model of SAS4A/SASSYS-1 predicted the delay of the outlet temperature drop but had major deviations from experimental data for the temperature distribution in the test vessel due to the limited number of representative temperature values. The 1-D mixing model of SAM showed good performance in predicting the outlet temperature evolution but had deviations in the temperature distribution as compared to measured

data. CFD had good agreement in predicting the slope but showed an earlier onset time of the outlet temperature evolution as compared to the measured data.

For Exp273, the perfect mixing model of SAS4A/SASSYS-1 did not perform well in prediction of both the temperature distribution of the test vessel sodium and the sodium outlet temperature evolution. The stratified volume model of SAS4A/SASSYS-1 did not properly capture the thermal stratification phenomena, as it didn't predict the timing of the outlet temperature drop as well as showing large deviations with the measured data. The 1-D axial mixing model of SAM showed good agreement in both aspects with a minor deviation in temperature distribution as compared to measurements, as the internal flow through UIS was not considered. CFD showed good performance in predicting the slope but showed an earlier onset time of the outlet temperature evolution as compared to the measured data.

For Exp270, the perfect mixing model of SAS4A/SASSYS-1 did not capture the thermal stratification phenomena. The stratified volume model of SAS4A/SASSYS-1 predicted the delay of the outlet temperature drop but had major deviations compared to the experimental data for temperature distribution in the test vessel due to the limited number of representative temperature values. The 1-D axial mixing model of SAM showed good agreement in temperature distribution and outlet temperature evolution. Minor deviations in temperature distribution were shown with measurements as the internal flow through UIS was not considered. CFD showed good performance in predicting the slope of temperature drop and coolant temperature in the test vessel but showed an earlier onset time of the outlet temperature evolution as compared to the measured data.

For Exp 277, the perfect mixing model and the stratified volume model of SAS4A/SASSYS-1 did not perform well, having large deviations in both the temperature distribution of sodium in the test vessel and the outlet temperature as compared to measured data. The 1-D axial mixing model of SAM showed good agreement in predicting outlet temperature evolution, but a higher slope of temperature drop was shown compared to the experimental data. CFD did not capture the temperature distribution of sodium in the test vessel and the outlet temperature evolution very well.

For Exp 283, the perfect mixing model of SAS4A/SASSYS-1 did not perform well in predicting outlet temperature evolution but had reasonable agreement with the temperature distribution of sodium in the test vessel. The stratified volume model of SAS4A/SASSYS-1 showed good agreement in prediction of the delay of the outlet temperature drop but had large local deviations due to the stepwise changes in temperature distributions caused by the coarse representation of the test vessel temperature layers. The 1-D axial mixing model of SAM performed well in predicting outlet temperature evolution but predicted higher slopes and earlier onset of drops of temperatures in the test vessel. CFD showed good agreement in both outlet temperature and coolant temperature distribution in the test vessel.

Table V Summary of the TSTF benchmark by fidelity levels and their qualitative performance

Code			SAS4A/SASSYS-1		SAM	CFD (STAR-CCM+)
Model			Perfect mixing model	Stratified volume model	1D axial mixing model	URANS
Fidelity level			0-D	0-D with sublayers	1-D	3-D
Exp.	UIS	Flow rate	Performance			
129	No	Low	Poor	Good	Good	Poor
133	No	High	Very good	Poor	Poor	Very good
224	Solid	Low	Poor	Good	Good	Good
227	Solid	High	Poor	Good	Good	Good
273	Variable – $\alpha=4\%$	Low	Poor*	Poor*	Very good*	Good
270	Variable – $\alpha=4\%$	High	Poor*	Good*	Very good*	Very good
277	Variable – $\alpha=100\%$	Low	Poor*	Poor*	Good*	Poor
283	Variable – $\alpha=100\%$	High	Good*	Good*	Good*	Very good

* Internal flow through the UIS was not modeled in the SAS4A/SASSYS-1 and SAM models for the variable UIS cases. This performance evaluation may change if the influence of internal UIS flow was included.

It should be noted that the assessment of each model was based on the TSTF benchmark results only. For instance, regarding the existence of an internal structure or obstruction, more sophisticated models are required for estimating jet penetration length, momentum transfer between the jet and the pool, and/or large temperature gradient at certain locations to accurately predict thermal stratification phenomena. Although the TSTF test vessel was designed to simulate the ABTR upper plenum by matching representative nondimensional numbers, its geometric specifications might affect the temperature distribution of sodium in the test vessel more than expected for the upper plenum for actual reactor conditions. In addition, as the TSTF operated in forced flow conditions, this assessment might be limited in prediction of the natural convection flow induced by temperature differences associated with thermal stratification.

5.2 Discussions on Thermal Stratification Models

Based on the TSTF benchmark computational results, models used in the present study are discussed here in terms of the model's capability to predict the plenum outlet temperature, typically the IHX inlet temperature.

The stratified volume model of SAS4A/SASYSS-1 has the capability to predict the evolution of stratified layer(s) using a small number of representative sublayers. The stratified volume calculation has the ability to include treatment of wall heat transfer for structures of interest. Therefore, it can provide the temperature of components that might be impacted by thermal stratification if they are explicitly treated in the model. However, because SAS4A/SASSYS-1 is based on the lumped approach in calculating pool temperatures, it has discretization limitations due to its coarse representation of stratified layers. This modeling artifact has been observed in predictions of step changes of the IHX primary side inlet temperature in other studies [14].

The 1-D axial mixing model of SAM showed good performance and the closest results to the CFD results among other computational models in the TSTF benchmark. As its simplified model originated as a model to predict thermal mixing phenomena, refinement of the model may be required to better capture thermal stratification, which may be dependent on the applications of use. For example, as the mixing mass flux was modeled by solving an additional momentum equation for the mixing velocity for the 1-D axial mixing model, a high-fidelity CFD simulation could assist in the development of a closure model [11].

CFD results of the TSTF benchmark did not show significant improvement in predicting trends relative to the other methods despite the utilization of detailed geometries and higher overall fidelity. Shortcomings of URANS have been addressed from the Reynolds analogy used to simplify turbulent heat flux where a consequent model error is introduced particularly in a heated boundary layer in non-unity Prandtl number fluid [15]. To compensate for its limitation, a recent study has performed the assessment of an advanced turbulence model in applying the prediction of the sodium stratified flow with a reasonable computational cost [16]. In addition, coupling a CFD code to a whole plant systems analysis code can potentially address limitations of the 0-D and 1-D methods, where CFD is utilized to model portions of the domain to avoid the excessive computational burden [17].

The representative computational models discussed in the present work have the potential to be useful during various stages of reactor design and licensing. For instance, the system level approach could be applied for safety calculations to obtain overall reactor behavior in transients. The 1-D model could support system level code calculations with relatively low computational cost but fair accuracy in predicting the temperature field in the domain of interest. CFD could be utilized to investigate and optimize the potential design of components of interest. Ultimately, it is most important to note that limitations of each model were largely dependent on experimental conditions and the utility of the computational model to appropriately treat those experimental conditions. Given this, it is vital for the end-user to fully understand the application domain, the physics that should be considered, and the ability of the computational tool to address those physics in the given application domain.

Acknowledgement

This work was sponsored by the U.S. Department of Energy's Office of Nuclear Energy (NE) and Office of Clean Energy Demonstrations (OCED) as part of the Advanced Reactor Demonstration Program. This work has been completed under ANL CRADA DE-AC02-06CH11357 and DOE DE-NE0009054.

References

1. D. Tenchine, "Some Thermal Hydraulic Challenges in Sodium Cooled Fast Reactors," *Nuclear Engineering and Design*, 240, p. 1195 (2010).
2. J. Schneider, M. Anderson, E. Baglietto, S. Bilbao y Leon, P. Brooks, M. Bucknor, C. Lu, M. Weathered, Z. Wu, and L. Xu, "Sodium Cooled Fast Reactor Key Modeling and Analysis for Commercial Deployment," NEUP 16-10268 Final Report, 2020.
3. C. Tomchik, P. Vegendla, M. Bucknor, J. A. Schneider, M. Anderson, "Benchmark Specification for Select Experiments Conducted at the University of Wisconsin-Madison Thermal Stratification Test Facility," Argonne National Laboratory, ANL-ART-253, August 2022.
4. Z. Wu, C. Lu, S. Morgan, S. Bilbao y Leon, M. Bucknor, "A status review on the thermal stratification methods for Sodium-cooled Fast Reactors," *Progress in Nuclear Energy*, 125, 103369 (2020).
5. T. H. Fanning, A. J. Brunett, T. Sumner, eds., "The SAS4A/SASSYS-1 Safety Analysis Code System," Argonne National Laboratory, ANL/NE-16/19, March 2017.
6. R. Hu, "SAM Theory Manual," Argonne National Laboratory, ANL/NE-17/4, March 2017.
7. C. J. Permann et al., "MOOSE: Enabling massively parallel Multiphysics simulation," *SoftwareX*, Vol. 11, 100430, 2020.
8. Siemens, Simcenter STAR-CCM+, v 2202.1 User Guide, 2020.
9. J. J. Lorenz, P. A. Howard, "Entrainment by a Jet at a Density Interface in a Thermally Stratified Vessel," *Transactions of the ASME*, 101, p. 539 (1979).
10. J. W. Yang, "Penetration of a Turbulent Jet with Negative Buoyancy into the Upper Plenum of an LMFBR," *Nuclear Engineering and Design*, 40, p. 297 (1977).
11. R. Hu, Y. Zhu, A. Kraus, "Advanced Model Developments in SAM for Thermal Stratification Analysis", ANL/NSE-18/7, September 2018.
12. W. M. Kay, "Turbulent Prandtl Number – Where Are We?," *Journal of Heat Transfer*, 116(2), p. 284 (1994).
13. R. Hu, L. Zou, G. Hu, T. Mui, "SAM User's Guide," Argonne National Laboratory, ANL/NSE-19/18 Rev. 1, February 2021.
14. International Atomic Energy Agency (IAEA), "Benchmark analyses on the natural circulation test performed during the PHENIX end-of-life experiments: final report of a co-ordinated research project 2008-2011," IAEA-TECDOC-1703 (2013).
15. T. Muramatsu, H. Ninokata, "Investigation of turbulence modelling in thermal stratification analysis," *Nuclear Engineering and Design*, 150, p. 81 (1994).
16. R. Wiser, E. Baglietto, J. Schneider, M. Anderson, "Validation of URANS and STRUCT- ϵ turbulence models for stratified sodium flow," *Nuclear Engineering and Design*, 399, 112009 (2022).
17. J. W. Thomas, T. H. Fanning, R. Vilim, L. L. Briggs, "Validation of the integration of CFD and SAS4A/SASSYS-1: Analysis of EBR-II Shutdown Heat Removal Test 17," *Proceedings of International Congress on the Advances in Nuclear Power Plants (ICAPP 2012)*, Chicago, June 24-28 (2012).

APPENDIX

This section includes the template of the SAS4A/SASSYS-1 TSTF model using stratified volume model– variable UIS (Exp270). Strings starting with ‘@’ notation are the placeholders for parameters listed in Table VI, which can be adjusted for each individual conditions in the parametric sensitivity analysis as described in Section 4.2.1. Note that the core model for SAS4A/SASSYS-1 TSTF model might contain values borrowed from the ABTR example inputs to complete the model required for SAS4A/SASSYS-1 run, but they should not impact on the benchmark results as the model focused on the test vessel.

Table VI A list of the parameters in the script used for sensitivity analysis

Parameters	Descriptions
@ICVST	Jet (coolant inlet) orientation – vertical (1) or horizontal (2)
@EPSTST	Minimum temperature difference for switching stages [K]
@XLENTR	Entrainment length [m]

```

#-----1-----2-----3-----4-----5-----6-----7-----8
#
Thermal Stratification Testing Facility (TSTF)
Simple loop geometry, Variable UIS
#-----1-----2-----3-----4-----5-----6-----7-----8
#
# STORAGE ALLOCATION RECORDS
#
#   NCH: Number of Channels
#   | NEUTSP: Neutronics Storage Allocation Flag
#   | | IDBUGP: Data Management Print Flag
#   | | | IPDECK: Input Data Editing Flag
#   | | | | NBYSSH: Number of Bypass Channels in SA-to-SA Heat Transfer
#   | | | | | IDATMO: Data Management Option Flag (0/1=Default/Extended)
#   | | | | | | IADEFEC: Data Pack DEFC Storage Allocation Flag
#   | | | | | | | IAPLUC: Data Pack PLUC Storage Allocation Flag
#   | | | | | | | | IACNTL: Control System Module Storage Allocation Flag
#   | | | | | | | | | IALBOP: BOP Module Storage Allocation Flag
#   | | | | | | | | | |
#   1 0 0 0 0 1 1 1 1 1
#
#-----1-----2-----3-----4-----5-----6-----7-----8
#
# INPCOM: Channel Independent Variables (Integer)
#
INPCOM      1      0      0
#
#           ICLCMP: Flag to Save Plot Data for Transients to Unit 11
#           |
#   24      1      1
#
#   -1
#-----1-----2-----3-----4-----5-----6-----7-----8

```

```

#
# OPCIN: Channel Independent Variables (Floating Point)
#       Time Steps and Convergence Criteria Data
#
OPCIN      11      0      0
#
#               EPSTEM: Steady-State Temperature Convergence
#               |
#       1      1      1.0E-03
#
#               DT0: Initial and Max Main Time Step Size
#               |
#       5      1      0.1
#
#               DTFUEL: Max Fuel Temp Change per Heat-Transfer Time Step
#               |               DTCLAD: Max Clad Temp Change per HT Time Step
#               |               |
#       10     2      5.0      30.0
#
#       -1
#-----1-----2-----3-----4-----5-----6-----7-----8
#=====
#
#               #####  #####  #####  #####
#               # # # # # # # # # #
#               # # # # # # # #
#               # # # ##### #####
#               # # # # # #
#               # # # # # #
#               #####  #####  #  #####
#
#               #####  #####  #  #  #####  #####
#               # # # # # # # # # # # #
#               # # # # # # # # # # # #
#               #####  # # # # # # # # # #
#               # # # # # # # # # # # #
#               # # # # # # # # # # # #
#               # # # # # # # # # # # #
#               # # # # # # # # # # # #
#
#-----1-----2-----3-----4-----5-----6-----7-----8
POWINA     12      1      1
#
#               POWTOT: Total Reactor Power (Watts)
#               |
#       3      1      0.0
#
#               FRPR: Fraction of Total Power Represented by All Channels
#               |               FRFLOW: Fraction of Total Flow Represented
#               |               |               by All SAS4A Channels
#       69     2      1.0      1.0
#
#       -1
#-----1-----2-----3-----4-----5-----6-----7-----8
#=====
#
#               #####  #  #  #####  #
#               # # # # # # # # # # # #
#               # # # # # # # # # # # #
#               #####  #  #####  #
#               # # # # # # # # # # # #

```



```

#---+---1---+---2---+---3---+---4---+---5---+---6---+---7---+---8
INPCOM      1      1      1
#
#           NCHAN: Number of Channels
#           |
#      1      1      1
#
#      -1
#---+---1---+---2---+---3---+---4---+---5---+---6---+---7---+---8
#
# INPCHN: Channel-Dependent Input (Integer)
#
INPCHN      51      1      0
#
#           IDBUGV: 8 for coolant-cladding temperature calculations
#           |
#      1      1      8
#
#           NPLN: Number of Segments in Gas Plenum
#           |           NREFB: Number of Reflector Zones below Pin
#           |           |           NREFT: Number of Reflector Zones above Pin
#           |           |           |           (Note: Below + Above <= 6)
#      4      3      1      1      1
#
#           NZNODE(KZ): Number of Segments in Zone KZ
#           |           |           |
#      7      3      1      5      1
#
#           NT: Number of Radial Temperature Nodes in Fuel
#           |
#      14     1      5
#
#           IFUELV: Table Number of Property Value for Driver Fuel
#           |           IFUELB: Table Number of Property Value for Blanket Fuel
#           |           |           ICLADV: Table Number for Cladding
#           |           |           |
#      15     3      1      0      1
#
#           NPIN: Number of Pins per Assembly
#           |           NSUBAS: Number of Subassemblies in Channel
#           |           |
#      25     2      1      1
#
#           IRHOK: 0 for tabular fuel thermo-physical properties
#           |
#      3      1      0
#
#      -1
#---+---1---+---2---+---3---+---4---+---5---+---6---+---7---+---8
#
# GEOMIN: Geometry Input for Channel (Floating Point)
#
GEOMIN      61      1      0
#
#           ACCZ(KZ): Coolant Flow Area per Fuel Pin in Zone KZ
#           |           |           |
#      1      3      1.2668E-04  2.0986E-04  3.8003E-04
#
#           AXHI(J): Length of Axial Segment J in Core and Blanket
#           |           |           |           |

```

```

      8      4      0.1      0.1      0.1      0.1
#
#           DHZ(KZ): Hydraulic Diameter for Zone KZ
#           |           |           |
# 32      3      1.27E-02      1.27E-02      1.27E-02
#
#           DSTIZ(KZ): Thickness of Inner Structure Node in Zone KZ
#           |           |           |
# 39      3      1.0E-06      1.0E-06      1.0E-06
#
#           DSTOZ(KZ): Thickness of Outer Structure Node in Zone KZ
#           |           |           |
# 46      3      1.0E-06      1.0E-06      1.0E-06
#
#           PLENL: Length of Fission-Gas Plenum
#           |
# 53      1      1E-06
#
#           RBR(J): Cladding Inner Radius for Axial Segment J
#           |
# 54      1      3.480E-03
#
#           RER(J): Cladding Outer Radius for Axial Segment J
#           |
# 78      1      4.000E-03
#
#           RBRPL: Cladding Inner Radius in Fission-Gas Plenum
#           |
# 102     1      3.480E-03
#
#           RERPL: Cladding Outer Radius in Fission-Gas Plenum
#           |
# 103     1      4.000E-03
#
#           RINFP(J): Fuel Inner Radius for Axial Segment J
#           |
# 104     1      0.0E+00
#
#           ROUTFP(J): Fuel Outer Radius for Axial Segment J
#           |
# 128     1      3.480E-03
#
#           ZONEL(KZ): Length of Zone KZ
#           |           |           |
# 152     3      0.1      0.4      0.064
#
#           SRFSTZ(KZ): Structure Perimeter per Pin in Zone KZ
#           |           |           |
# 159     3      3.9898E-02      6.5031E-02      1.1969E-01
#
#           AREAPC: Coolant Plus Pin Area per Pin in the Pin Section
#           |
# 166     1      3.3654E-04
#
#           RBR0: Nominal Cladding Inner Radius
#           |           RER0: Nominal Cladding Outer Radius
#           |           |
# 180     2      3.480E-03      4.000E-03
#
#

```

```

#
# SER(KZ): Reflector Perimeter, Pin Perimeter in Plenum
Region
#
# 182 3 1.0E-06 2.5133E-02 1.0E-06
#
# DRFO(KZ): Thickness of Outer Reflector Node/Cladding
#
# 169 3 1.0E-06 5.2E-04 1.0E-06
#
# DRFI(KZ): Thickness of Inner Reflector Node in Zone KZ
#
# 189 3 1.0E-06 0.0 1.0E-06
#
# -1
#-----1-----2-----3-----4-----5-----6-----7-----8
#
# POWINC: Channel-Dependent Power Input (Floating Point)
#
# POWINC 62 1 0
#
# GAMSS: Fraction of Power from Direct Heating of Structure
#
# 2 1 1.0E-10
#
# GAMTNC: Fraction of Power from Direct Heating of Coolant
# GAMTNE: Fraction of Heating in Cladding
#
# 4 2 1.0E-10 1.0E-10
#
# PSHAPE(J): Ratio of Pin Power in Axial Segment J to Peak.
#
# 6 4 1.00 1.00 1.00 1.00
#
# PSHAPR(I): Radial Power Shape within Pin
#
# 30 5 1.0E+00 1.0E+00 1.0E+00 1.0E+00 1.0E+00
#
# PRSHAP: Ratio of Average Power per Subassembly to Average
Power
# Over All Subassemblies
#
# 256 1 1.0
#
# -1
#-----1-----2-----3-----4-----5-----6-----7-----8
#
# PMATCH: Channel-Dependent Properties Input (Floating Point)
#
# PMATCH 63 1 0
#
# XKSTIZ(KZ): Inner Structure Thermal Conductivity for Zone
KZ
#
# 11 3 26.0 26.0 26.0
#
# XKSTOZ(KZ): Outer Structure Thermal Conductivity for Zone
KZ
#
# 18 3 26.0 26.0 26.0
#

```



```

1      2      0.017 0.000000001
#
#          C1, C2, C3: Coefficients for Convection Heat-Transfer
Coefficient
#          |          |          |
#      3      3      2.5E-02      8.0E-01      4.8E+00
#
#          DWMAX: Maximum Fraction Change in Coolant Flow Rate per
#          |          Heat-Transfer Time Step before Boiling
#      6      1      0.2
#
#          RELAM: Re Number for Switch between Turb. and Laminar
Friction Factor
#          |          AFLAM: Laminar Friction Factor = AFLAM/Re
#          |          |
#      7      2      2000.0      64.0
#
#          W0: Steady-State Coolant Flow Rate per Pin
#          |
#      47      1      0.4738
#
#          XKORV: Orifice Coefficient at the bottom of each zone
#          |
#      48      1      300.0
#      49      1      0.0
#      50      1      0.0
#
#          DZIAB, DZIAT: Effective Coolant Inertial Term Below/Above
#          |          |          Subassembly Inlet/Outlet
#      65      2      318.31      318.31
#
#          THETA1, THETA2: 0.5 Normally, 0/1 for Implicit Calculation
#          |          |
#      67      2      0.5      0.5
#
#          DTLMAX: Maximum Coolant Temperature Change per Coolant Time
Step
#          |
#      69      1      15.0
#
#          DTCMIN: Minimum Coolant Time Step Size before Boiling
#          |
#      171      1      1.0E-05
#
#      -1
#
#-----1-----2-----3-----4-----5-----6-----7-----8
#=====
#
#          #####      #####      ###      #      #      #      #####
#          #      #      #      #      #      ##      ##      #      #      #
#          #      #      #      #      #      #      #      #      #      #
#          #####      #####      #      #      #      #      #      #####
#          #      #      #      #      #      #      #####      #      #
#          #      #      #      #      #      #      #      #      #      #
#          #      #      #      ###      #      #      #      #      #
#
#-----1-----2-----3-----4-----5-----6-----7-----8
INPCOM      1      1      1
#

```

```

#           NPRES: Coolant driving pressure option
#           |           Negative value for # of entries in table of normalized
flow rate vs. time.
#           |
#   19      1      -1
#
#           NTOTAB: Number of entries in TOTAB vs. TOTME table of
#           |           coolant inlet temperature vs. time.
#   22      1      1
#
#           IPRION: PRIMAR-4 Option Flag
#           |
#   27      1      0
#
#   -1
#-----1-----2-----3-----4-----5-----6-----7-----8
#
# OPCIN: Channel Independent Variables (Floating Point)
#           Time Steps and Convergence Criteria Data
#
OPCIN      11      1      1
#
#           DTP0: Initial PRIMAR Time Step Size
#           |           DTPMAX: Maximum PRIMAR Time Step Size Before
#           |           Boiling Starts
#   13      2           0.25      0.25
#
#   -1
#-----1-----2-----3-----4-----5-----6-----7-----8
PRIMIN     14      0      0
#
#           PX: Coolant Exit Pressure at ZPLENU
#           |
#   1       1       7.0E+04
#
#           PRETAB: Normalized inlet coolant driving pressure or
coolant flow rate
#           |           at times listed in PRETME
#           |
#   5       1           1.0
#
#           TOTAB(L): Inlet Temperature at Time TOTME(L)
#           |
#   45      1       570.50
#
#           ZPLENL/ZPLENU: Inlet/Outlet Plenum Reference Elevation
#           |           |
#   87      2       -0.1      1.7467
#
#   -1
#-----1-----2-----3-----4-----5-----6-----7-----8
#=====
#
#   #####   ###   #   #   #####   #####   #####   #####
#   #         #   ##  ## #           #   #   #   #   #   #
#   #         #   # # # # #           #         #   #   #   #
#   #         #   # # # #####         #####   #   #####   #####
#   #         #   #   # #           #         #   #   #

```

```

#           #           #           #           #           #           #           #           #
#           #           ###          #           # #####          #####          #           # #####          #
#
=====
INPCOM      1           1           1
#
#           IPOWER: 0/1 = Reactivity/Power vs Time from PREA
#           |
#      8      1           1
#
#           MAXSTP: Maximum Number of Main (Power and Reactivity)
#           |           Time Steps
#     11      1 99999
#
#           IPO: Number of Steps between Prints before IBLPRT or Boiling
#           |           IPOBOI: Number of Steps between Prints after IBLPRT or
Boiling
#           |           |
#     12      2           20           20
#
#           NPREAT: Number of Entries in PREA vs. Time Table
#           |           (Power or Reactivity vs Time)
#     18      1           4
#
#           NOREAC: Main Time Step Intevals between PSHORT Print
#           |
#     41      1           20
#
#           IFIT(K): Input Table Lookup Options (K=1: Power/Reac vs. Time)
#           |           (0=Linear Fit)
#     95      1           0
#
#     -1
#-----1-----2-----3-----4-----5-----6-----7-----8
POWINA     12           1           1
#
#           PREATB: Transient power table used by PREA
#           |           |           |           |
#     29      4           1.0           1.0           1.0           1.0
#
#           PREATM: Times for PREATB
#           |           |           |           |
#     49      4           0.0           10.0           30.0           1000.0
#
#     -1
#-----1-----2-----3-----4-----5-----6-----7-----8
OPCIN      11           1           1
#
#           DTMXB: Max heat transfer time-step after coolant boiling
inception
#           |
#     6      1           0.01
#
#           TIMAX: Maximum Problem Time (s)
#           |
#     7      1           238.75
#
#           TCOSTP: # of CPU seconds reserved at end of run for writing
restart files
#           |

```

```

9      1      15.0
#
#          DTPBOI: Max PRIMAR step size after start of boiling
#          |
15     1      0.01
#
#          DPINMX: Max change in inlet pressure per PRIMAR step
#          |          DTINMX: Max change in inlet temp per PRIMAR
step
#          |          |          DTMMXB: Max main time step after
onset of boiling
#          |          |          |
19     3      5.0E+03      5.0      0.5
#
#          DTMIN: Time Step Sizes vs. Time
#          |          |
95     2      0.25      0.25
#
#          TDTMIN: Time for Time Step Sizes
#          |          |
105    2      0.0      1000.0
#
-1
#
#-----1-----2-----3-----4-----5-----6-----7-----8
#
#-----1-----2-----3-----4-----5-----6-----7-----8
#
#####  #####  #  #      #      #      #####      #  #
#  #      #  #      #  #  #      #  #      #      #      #  #
#  #      #  #      #  #  #      #  #      #      #      #  #
#  #####  #####  #  #  #  #      #  #      #      #####  ###  #####
#  #      #  #      #  #      #  #      #####  #      #      #
#  #      #  #      #  #      #  #      #  #      #  #      #
#  #      #  #      #  #      #  #      #  #      #  #      #
#
#          #          #      #####  #####  #####  #
#          ##      ##  #      #  #      #      #      #
#          #  #      #  #      #  #      #  #      #      #
#          #  #  #      #  #      #  #      #      #####  #
#          #      #      #  #      #  #      #      #      #
#          #          #  #      #  #      #      #      #
#          #          #      #####  #####  #####  #####
#
#-----1-----2-----3-----4-----5-----6-----7-----8
#
#-----1-----2-----3-----4-----5-----6-----7-----8
#
INPCOM      1      1      1
#
#          IPRION: 4 triggers PRIMAR-4 option
#          |
27     1      4
-1
#
#-----1-----2-----3-----4-----5-----6-----7-----8
#
INPMR4      3      1      0
#
#          NCVP: # Compressible Volumes, Primary Loop

```

```

#           |           NCVS: # Compressible Volumes, Secondary Loop
#           |           |           NCVS: # CV in DRACS Loop
#           |           |           |           NSEGLP: # Liquid Segments, Primary Loop
#           |           |           |           |           NSEGLP: # Liquid Segments, Secondary Loop
#           |           |           |           |           |
#   1       5       3       0       0       3       0
#
#           NELEMT: Total # of Liquid Flow Elements
#           |
#   10      1      10
#
#           ITYPCV: Compressible Volume Type
#           1 = Inlet Plenum
#           4 = Almost incompressible liquid, no gas
#           7 = Outlet plenum with cover gas
#           8 = Pool with Cover Gas
#           |           |           |           |
#   11      3      1       7       4
#
#           ITYPEL: Liquid Flow Element Type
#           1 = Core Subassemblies
#           2 = Bypass Channel
#           3 = Pipe
#           5 = Pump Impeller
#           6 = IHX, Shell Side
#           11 = Valve
#
#           Core  Pipe  Pipe  Pipe  IHX  Pipe
#           |     |     |     |     |     |
#   49      6     1     3     3     3     6     3
#           Pipe  Pump  Pipe  Pipe
#           |     |     |     |
#   55      4     3     5     3     3
#
#           JCVL: Compressible Volumes at ends of Liquid Segments
#           |           |           |           |           |           |           |
#   189     2     1     2
#   191     2     2     3
#   193     2     3     1
#
#           NELML: # of Elements in Liquid Segment
#           |           |           |           |
#   325     3     1     5     4
#
#           JFSELL: First Element # in Segments
#           |           |           |           |
#   365     3     1     2     7
#
#           NPUMP: # of Sodium Pumps
#           |           IELPMP: Element # of Pump
#           |           |
#   405     2     1     8
#
#           IEMPMP: Type of Pump (IEMPMP = 2 is for Homologous Pump Model)
#           |           (IEMPMP = 0 is for table of pump head vs
time)
#   418     1     0
#
#           ILRPMP: Pump Operation Option
#           | (0 = pump operation according to model selected)

```

```

# | (1 = pump speed set to zero, locks rotor immediately as in a
pump seizure)
# | (-1 = for table of pump speed vs. time (IEMPMP 1 or 2))
# | (-2 = for table of pump head vs. flow)
# 430 1 0
#
# NIHX: Number of Intermediate Heat Exchangers
# |
# 470 1 1
#
# IELIHX: Element # of IHX in primary loop
# |
# 473 1 5
#
# ILIHXS: Element # of IHX in intermediate loops
# |
# 481 1 X
#
# IHXCLC: IHX Detailed or Simple model option
# | (0 = Use Detailed Model)
# | (1 = Use Simple Model)
# 489 1 -1
#
# IPRADJ: Inlet/Outlet Plena Pressure Adjustment Option
# |
# 497 1 1
#
# NTGPT: # of Temperature Groups
# |
# 512 1 7
#
# NTNODE: # of Nodes in the Temperature Group. 2 nodes for tabular
IHX.
# | | | | | | |
# 513 7 5 5 5 2 5 10 5
#
# IFSTEL: First Element in Temperature Group
# | | | | | | |
# 613 7 2 3 4 5 6 7 10
#
# ILSTEL: Last Element in Temperature Group
# | | | | | | |
# 713 7 2 3 4 5 6 9 10
#
# ISSIHX: Steady-state IHX temperature drop, if 1, user specifies
# |
# 1155 1 0
#
# ISSPMP: Steady-state pump head, if 1, user specifies
# |
# 1159 1 0
#
# IPIPTM: Pipe Temp Convection Differencing Approx. (Recommended =
2)
# | Multiple Inlet/Outlet Plenum Option
# | |
# 1310 2 2 0
#
#####
#

```

```

# Fort.15 output for PRIMAR-4
#
# IP4PRT: How many PRIMAR steps to print PRIMAR-4 results
# | NBINOT: # of IBINOT entries for PRIMAR-4 on unit 15
# | | IBINST: How many IBINST steps between PRIMAR-4 binary
output
# | | |
# 890 3 20 13 1
# 893 1240001 Inlet Plenum Temperature
# 894 1240002 Outlet Plenum Temperature
# 895 1240003 Reservoir Temperature
#
# 896 1010001 Core Flow Rate
# 897 1010002 Downstream Flow Rate
# 898 1010003 Upstream Flow Rate
#
# 899 1160001 Inlet Plenum Pressure
# 900 1160002 Outlet Plenum Pressure
# 901 1160003 Reservoir Pressure
#
# 902 1300402 Outlet Temperature
# 903 1280101 TS inlet Temperature
# 904 1300410 E10 Temperature
#
# 905 1190002 Outlet Plenum cover gas interface height
#
#####
#
#####
# Stratified Compressible Volumes
#####
#
# NSTRCV: Number of stratified compressible volumes
# | ICVSTR: Compressible volume number for stratified treatment
# | |
# 1313 2 1 2
#
# ISTRVT: 1 for vertical coolant inlet, as in an outlet plenum
# | 2 for a horizontal coolant inlet
# 1317 1 @ISTRVT
#
# NUMWAL: Number of wall sections
# |
# 1320 1 1
#
# IFSTWL: Wall number (IW) of the first wall section
# | |
# 1323 1 1
#
# NVNDWL: Number of vertical nodes in a vertical wall
# | Input 1 for a horizontal wall
# |
# 1335 1 10
#
# NLNDWL: Number of lateral nodes in a wall section
# |
# 1344 1 5
#
# ICV2WL: Number of the CV in contact with the outer side of the
wall section

```

```

#
# 1353      1      |
#
#           ISTDBS: PRIMAR time step when stratified debug starts
#           |
# 1363      1      1
#
#           IFT16: Write out stratified CV output to STRATCV.dat
#           |
# 1365      1      1
#
# -1
#
#-----1-----2-----3-----4-----5-----6-----7-----8
#
PMR4IN      18      1      0
#
#####
# Liquid Segment Data
#####
#
#           FLOSSL: Initial flow rate in liquid flow segments.
# Important for convergence.
#           |           |           |
# 2         3         0.4738      0.4738      0.4738
#
#           ZINL: Height of inlet to the liquid segment
#           |           |           |
# 42        3         -0.1        1.291        -1.0
#
#           CVLMLT: Multiplicity Factors at Liquid Segment Ends
#           |           |           |           |
# 82         2         1.0         1.0         Segment 1 (Core in / out)
# 84         2         2.0         1.0         Segment 2 (Outlet / CV3 in)
# 86         2         0.5         1.0         Segment 3 (CV3 out / CV1 in)
#
#####
# Liquid Element Data
#####
#
#           ZOUTEL: Height at Outlet of the liquid element
#           |           |           |           |           |
# 162        5         0.464        1.291        0.4         1.908        0.4
# 167        5         -0.5        -1.0        -1.0        -1.0        -0.5
#
#           XLENEL: Liquid element length
#           |           |           |           |           |
# 302        5         0.564        0.14764       0.891        1.96036       1.508
# 307        5         0.9         0.2         0.1         0.2         0.5
#
#           AREAEL: Cross-sectional flow area of liquid elements
#           |           |           |           |           |
# 442        5         3.8003E-04  1.9793E-04  1.9793E-04  1.9793E-04  1.9793E-04
# 447        5         5.0671E-04  5.0671E-04  5.0671E-04  5.0671E-04  5.0671E-04
#
#           DHELEM: Hydraulic Diameter of liquid elements
#           |           |           |           |           |
# 582        5         0.0127       0.015875   0.015875   0.015875   0.015875
# 587        5         0.0254       0.0254     0.0254     0.0254     0.0254
#
#

```

```

#          ROUGH1: Pipe Surface Roughness
#          |          |          |          |          |
# 722      5      1.0E-05      1.0E-05      1.0E-05      1.0E-05      1.0E-05
# 727      5      1.0E-05      1.0E-05      1.0E-05      1.0E-05      1.0E-05
#
#          BENDNM: Number of Bends in Each Liquid Element
#          |          |          |          |          |
# 862      5          0.0          0.0          0.0          1.0          0.0
# 867      5          0.0          0.0          0.0          0.0          0.0
#
#          G2PRDR: Initial Orifice Coefficient, normally 0 as input
#          |          |          |          |          |
# 1002     5          0.0          0.0          0.0          0.0          0.0
# 1007     5          0.0          0.0          0.0          0.0          0.0
#
#          BNDL0D: Effective L/D per bend
#          |
# 1142     1          15.0
#
#          WALLMC: Pipe wall mass times heat capacity/length
#          |          |          |          |          |
# 1143     5          1.0          1.0          1.0          1.0          1.0
# 1148     5          1.0          1.0          1.0          1.0          1.0
#
#          WALLH: Pipe wall heat transfer coefficient
#          |          |          |          |          |
# 1283     5          1.0          1.0          1.0          1.0          1.0
# 1288     5          1.0          1.0          1.0          1.0          1.0
#
#####
# Compressible Volume Data
#####
#
#          VOLLGC: Total Volume of Compressible Volumes
#          |          |          |
# 1423     3  7.6006E-04  9.0283E-02  7.6006E-04
#
#          VOLGS0: Initial Gas Volume
#          |          |          |
# 3612     3          0.0  1.0018E-02          0.0
#
#          PRES00: Initial Gas Pressure in CV
#          |          |          |
# 1461     3          0.0  7.0E+04          0.0
#
#          ALPHAP: CV volume pressure expansion coefficient
#          |          |          |
# 1499     3  1.00000E-07  1.00000E-07  1.00000E-07
#
#          ALPHAT: CV volume thermal expansion coefficient
#          |          |          |
# 1537     3  2.0E-05      2.0E-05      2.0E-05
#
#          ZCVL: CV reference height for liquid pressure
#          |          |          |
# 1575     3          -0.5          0.464          -1.0
#
#          AREAIN: Liquid-Gas Interface Area in CV
#          |          |          |
# 1613     3          0.0  6.2109E-02          0.0

```

```

#
#           TREFCV: Steady-state gas temperature in CV
#           |           Input as 0.0 to use liquid temperature
#           |           |           |
1651      3           0.0           0.0           0.0
#
#           BTAPNA: Sodium isothermal compressibility for the CV
#           |           |           |
2464      3           2.0E-10        2.0E-10        2.0E-10
#
#           BTATNA: Sodium thermal expansion coefficient for the CV
#           |           |           |
2502      3           3.0E-04        3.0E-04        3.0E-04
#
#           HWALL: Wall-coolant heat-transfer coefficient for CV
#           |           |           |
2578      3           1.0           1.0           1.0
#
#           AWALL: Wall surface area
#           |           |           |
2616      3           7.9796E-03      2.0517E+00      7.9796E-03
#
#           CMWALL: CV Wall mass times specific heat
#           |           |           |
2654      3           1.0           1.0           1.0
#
#####
# Simple Pump Data
#####
#
# Pump Input:
# For IEMPMP = 0
#
#           APMPHD: Table of Relative Pump Head
#           |           |           |           |           |
1983      5           1.0           1.389          1.389          1.0E-3          1.0E-3
#
#           AMOTK: Table of Relative Pump Head
#           |           |           |           |           |
2223      5           0.0           8.0           233.8          235.0          1000.0
#
#           GRAVTY: Acceleration due to gravity
#           |
2463      1           9.8
#
#####
# Simple IHX Model Data
#####
#
#           DTMPTB: Table of normalized temperature drop for IHX
#           |           |           |           |           |
2937      5           575.508        575.508        566.0          522.2          493.0
2942      4           480.0          475.9          475.7          475.7
#
#           ZCENTR: Height of thermal center for IHX
#           |           |           |           |           |
3105      5           1.154          1.154          1.154          1.154          1.154
3110      4           1.154          1.154          1.154          1.154
#
#           TMPMTB: Times for DTMPTB and ZCENT

```

```

#           |           |           |           |
# 3273      5           0.0           1.0           1.5           3.0           8.0
# 3278      4           18.0          40.0          215.0          1000.0
#
#           C1PIPE, C2PIPE, C3PIPE: Conductance coefficient for pipe,
# recommended values
#           |           |           |
# 3650      3           0.025          0.8           4.80
#
#           EPSF: Maximum fractional change in liquid segment flow rate
# per time step
#           |           |           |
#           EPSFC: Maximum fractional change in core inlet
# flow rate
#           |           |           |           |           |
#           |           |           |           |           |           |
# 4282      2           0.2           0.1           |           |           |
#
#####
# Cover Gas Data
#####
#
#           GAMGSC: Cp/Cv for cover gas
#           |
# 1689      1           1.4 # for N2 gas
#
#           RGASC: Gas constant for cover gas. 208.1 for argon gas.
#           |
# 1690      1           296.8 # for N2 gas
#
#           U0CVGS: Cover gas viscosity
#           |
# 1691      1 1.7562E-05 # for N2 gas
#
#           TRFU: Gas viscosity reference temperature
#           |
# 1692      1           293.0
#
#           TAUGAS: Cover-gas temperature time constant.
#           |           |           |
# 1861      3           0.0           100.0          0.0
#
#####
# Stratified Compressible Volume
#####
#
#           RCORE: Core radius for use in the Richardson number
#           |
# 5008      1           0.035
#
#           HCSTWL: Coolant heat transfer coefficient at the inner
# surface
#           |           |           |
#           |           |           |           |
# 5009      1           1.0
#
#           HCSTW2: Coolant heat transfer coefficient at the outer
# surface
#           |           |           |
#           |           |           |           |
# 5018      1           0.0
#

```

```

#          ASTWL: Area of the wall section
#          |
# 5027      1  2.0517E+00
#
#          HINVWL: Thickness/thermal conductivity of node I in the
wall section
#          |          |          |          |          |
# 5036      5  7.62000E-04 7.62000E-04 7.62000E-04 7.62000E-04 7.62000E-04
# 5044      5  7.62000E-04 7.62000E-04 7.62000E-04 7.62000E-04 7.62000E-04
#
#          XMCSTW: Mass × heat capacity of node I in the wall
#          |          |          |          |          |
# 5108      5  9.93310E+03 9.93310E+03 9.93310E+03 9.93310E+03 9.93310E+03
# 5116      5  9.93310E+03 9.93310E+03 9.93310E+03 9.93310E+03 9.93310E+03
#
#          ZINST : z of inlet (only used for vertical inlet)
#          |
# 5180      1      0.4544
#
#          EPSTST: Minimum temperature difference for switching stages
#          |
# 5186      1      @EPSTST
#
#          XLENTR: Entrainment length
#          |
# 5189      1      @XLENTR
#
#####
# Initial Conditions
#####
#
#          TPLCV: Temperature of CV. Entered only for inlet plena
#          |
# 4685      1      575.50
#
#          PPLCV: CV pressure for outlet plena only
#          |
# 4724      1      7.0E+04
#
#          ZPLENC: CV reference elevation for plena only
#          |          |
# 4761      2      -0.1      1.7467
#
# -1
#
#-----1-----2-----3-----4-----5-----6-----7-----8
#####
ENDJOB      -1
#####
#-----1-----2-----3-----4-----5-----6-----7-----8

```




Nuclear Science and Engineering Division

Argonne National Laboratory
9700 South Cass Avenue, Bldg. 208
Argonne, IL 60439

www.anl.gov



**U.S. DEPARTMENT OF
ENERGY**

Argonne National Laboratory is a U.S. Department of Energy
laboratory managed by UChicago Argonne, LLC